Local and systemic responses conferring acclimation of Brassica napus roots to low phosphorus conditions

Article

Accepted Version

Local and systemic responses conferring adaptation of *Brassica napus* roots to low phosphorus conditions

Yalin Li[1,2], Xinyu Yang[1,2], HaiJiang Liu[1,2], Wei Wang[1,2], Chuang Wang[1,2], Guangda Ding[1,2], Fangsen Xu[1,2], Sheliang Wang[1,2], Hongmei Cai[1,2], John P. Hammond[3], Philip J. White[1,4], Sergey Shabala[5,6], Min Yu[6], Lei Shi[1,2,*]

[1]National Key Laboratory of Crop Genetic Improvement, Huazhong Agricultural University, Wuhan 430070, China

[2]Microelement Research Center/Key Laboratory of Arable Land Conservation (Middle and Lower Reaches of Yangtze River), Ministry of Agriculture and Rural Affairs, Huazhong Agricultural University, Wuhan 430070, China

[3]School of Agriculture, Policy and Development, University of Reading, Reading RG6 6AR, UK

[4]The James Hutton Institute, Invergowrie, Dundee DD2 5DA, UK

[5]Tasmanian Institute of Agriculture, College of Science and Engineering, University of Tasmania, Hobart, Tas 7001, Australia

[6]International Research Center for Environmental Membrane Biology & Department of Horticulture, Foshan University, Foshan 528000, P.R. China

[*]**Correspondence**

Lei Shi, National Key Laboratory of Crop Genetic Improvement, Huazhong Agricultural University, Wuhan, China.

E-mail: leish@mail.hzau.edu.cn; Fax: +86 27 87280016

Running Head: Root plasticity of *B. napus* with heterogenous Pi availability

Summary: This work reveals the mechanistic basis of locally and systemically regulated responses of *B. napus* root architecture to heterogenous Pi distribution under in vitro conditions.

Abstract

Due to the non-uniform distribution of inorganic phosphate (Pi) in the soil, plants modify their root architecture to improve acquisition of this nutrient. In this study, a split-root system was employed to assess the nature of local and systemic signals that modulate root architecture of *Brassica napus* grown with non-uniform Pi availability. Lateral root (LR) growth was regulated systemically by non-uniform Pi distribution, by increasing the density of the second-order LR (2°LR) in compartments with luxury Pi supply but decreasing the 2°LR density in compartments with low Pi availability. Transcriptomic profiling identified groups of genes regulated, both locally and systemically, by Pi starvation. The number of systemically induced genes was greater than the number that was locally induced and included genes related to abscisic acid (ABA) and jasmonic acid (JA) signalling pathways, reactive oxygen species (ROS) metabolism, sucrose, and starch metabolism. Physiological studies confirmed the involvement of ABA, JA, sugars, and ROS in the systemic Pi starvation response. The data reported reveal the mechanistic basis of local and systemic responses of *B. napus* to Pi starvation and provide new insights into the molecular and physiological basis of root plasticity.

Key words: *Brassica napus*, heterogeneous Pi availability, local regulation, systemic regulation, abscisic acid, jasmonic acid, sugar, ROS, phosphate, phosphorus

Introduction

Phosphorus (P) is one of the most critical macronutrients for plant growth and development (Hawkesford *et al.*, 2012). Although the total content of P in the soil can be high, in many cases the availability of inorganic phosphate (Pi), the main form of P that can be taken up by plants, is limited. Pi can precipitate with calcium, magnesium, aluminium and iron, and the high sorption capacity of Pi to soil particles results in a very low availability and heterogeneous distribution in soil (Obersteiner *et al.*, 2013; Zhang *et al.*, 2013; Lynch and Wojciechowski, 2015; Jin *et al.*, 2017).

To counter these constraints, plants have evolved various adaptive strategies to detect Pi distribution in their environment and adapt their morphology and physiology to variations in Pi concentration (Williamson *et al.*, 2001; Lynch, 2011). Root system architecture (RSA) is highly plastic in response to the heterogenous distribution of Pi, with plants varying both the length and density of their primary (PR) and lateral (LR) roots and root hairs (Péret *et al.*, 2014; Bouain *et al.*, 2016; Gutiérrez-Alanís *et al.*, 2018). For example, shallow root systems have more LRs distributed in the topsoil for better acquisition of the poorly mobile Pi (Jin *et al.*, 2017; van der Bom *et al.*, 2020). This plasticity in RSA in response to localised Pi availability is highly species-specific. For example, in wheat and chickpea root proliferation was significantly increased in the Pi-enriched zone, whereas RSA in maize and faba bean were not responsive to local Pi availability (Li *et al.*, 2014). In *Arabidopsis*, localised Pi availability resulted in a significant increase in LR length in the Pi-enriched zone, whereas LR density was not affected (Linkohr *et al.*, 2002) or even decreased.

Modulation of RSA in response to Pi starvation is driven by two partially independent signalling pathways: local (confined to roots) and systemic (involving long-distance root-to-shoot and shoot-to-root communication) (Chien *et al.*, 2018; Ham *et al.*, 2018; Oldroyd and Leyser, 2020). Local

responses are modulated by the external Pi availability in the growth medium, while systemic responses depend on the internal Pi concentrations in the plant (Svistoonoff *et al.*, 2007; Lin *et al.*, 2014). The root cap is positioned at the very end of root tip and is responsible for sensing Pi availability (Svistoonoff *et al.*, 2007; Ticconi *et al.*, 2009; Ravelo‐Ortega *et al.*, 2022). Manipulating local Pi availability through split-root experiments mimics the heterogeneous Pi distribution in soil and allows changes in RSA and local and systemic responses to Pi starvation to be determined (Franco-Zorrilla, 2005; Thibaud *et al.*, 2010). At the same time, genome-wide transcriptome analysis has been successfully used to elucidate molecular mechanisms underlying complex adaptations of crops to Pi deficiency using the RNA-seq technique (Wang *et al.*, 2016; Xue *et al.*, 2018; Wang *et al.*, 2019). Combined, these two techniques provide an excellent tool to understand the mechanistic basis of modulation of RSA and the molecular nature of the local and systemic signals involved.

LOW PHOSPHATE ROOT1 and 2 (LPR1 and LPR2) proteins play a critical role in sensing local Pi availability in Arabidopsis, since LPR1 is expressed in the root cap (Svistoonoff *et al.*, 2007). PHOSPHATE DEFICIENCY RESPONSE 2 (PDR2) and LPR1 may function together in mediating responses of the root meristem to external Pi availability (Ticconi *et al.*, 2009; Ruiz-Herrera *et al.* 2015). Local low Pi sensing enhances auxin responses and involves Mitogen-Activated Protein Kinase 6 (MPK6) signalling within the root tip, particularly the root cap via SOMBRERO (Pérez-Torres *et al.*, 2008; López-Bucio *et al.*, 2019; Ravelo-Ortega *et al.*, 2022). In addition, the SENSITIVE TO PROTON RHIZOTOXICITY1 - MEDIATOR16 - ALUMINUM-ACTIVATED MALATE TRANSPORT1 (STOP1 - MED16 - ALMT1) signalling module is involved in root system remodelling in response to low Pi availability (Raya-González *et al.*, 2021; Ruiz-Herrera *et al.*, 2021). Most of the current knowledge comes from *Arabidopsis* plants and, in the light of the species-specificity of RSA responses to Pi starvation, direct translation of

some findings to other species is debatable.

Oilseed rape (*Brassica napus* L.) is one of the most important oil crops cultivated throughout the world and is extremely sensitive to Pi deficiency (Chen *et al.*, 2015). No study has investigated the nature of the local and systemic responses to Pi starvation in this species. In this work, we took advantage of the availability of high-quality genomic sequences of *B. napus* (Sun *et al.*, 2017; Song *et al.*, 2020) and utilised a split-root system to investigate local and systemic regulation of RSA in response to homogeneous and heterogeneous Pi availability in this species, both at transcriptional and functional levels.

Materials and methods

Split-root experiments

'ZhongShuang11 (ZS11)', a semi-winter *B. napus* cultivar used in this work, is the most popular cultivar grown in the middle and downstream regions of the Yangtze River basin. Seeds of 'ZS11' were kindly provided by the Oil Crops Research Institute, Chinese Academy of Agriculture Science. Seeds were surface sterilized in 1.0 % (v/v) NaClO for 20 min, rinsed five times in sterile distilled water, and then sown in sterile Petri dishes (13 × 13 × 1 cm) containing 60 mL Murashige–Skoog (MS) salt with 1.0 % (w/v) agar (Sigma-Aldrich, St. Louis, MO, catalogue no. A1296) and 625 μM KH_2PO_4 (+P). After 3 days, uniform *B. napus* seedlings were selected. The primary root tip was removed mechanically to induce the formation of lateral roots and allow the development of a split-root system. After another 3 d, seedlings with two lateral roots of the same length were transferred to the bigger (25 × 25 × 2 cm) sterile Petri dish (growth chamber) containing 110 mL MS with 1.0 % (w/v) agar. A thin plastic sheet was inserted to separate the chamber into two compartments, with contrasting Pi availability: (1) compartment containing 625 μM KH_2PO_4

(abbreviated as +P), and (2) 0 μM KH_2PO_4 (abbreviated as -P). In the latter case, KH_2PO_4 in MS media was replaced with KCl. The pH was adjusted to 5.6 in both compartments. One lateral root (LR) of the first order (1^o) was placed into the +P compartment (abbreviated hereafter as R+), and one was placed into the -P compartment (R-). For controls, chambers with uniform P distribution between compartments - either with 625 μM P supply in both compartments (abbreviated as R++) or without P (abbreviated as R--) were used. Each Petri dish contained two plants. Plants were grown in a controlled environment chamber with a photoperiod of 16 h of light and 8 h of darkness at 22~24 °C. The light intensity was 300-320 μmol $m^{-2}s^{-1}$ (photon flux density) and the relative humidity was 60-75%. Plants were photographed, and then shoots (S++, S+- and S--) and roots (R++, R+, R- and R--) were harvested after 9 d of treatment.

To check the effect of JA, ABA and sugars on plant responses to Pi availability in a split-root experiment, 1 μM JA, 10 μM DIECA (diethyldithiocarbamic acid, a JA biosynthesis inhibitor), 5 μM ABA, 3 μM FLD (fluridone, an ABA biosynthesis inhibitor), and 1% sucrose were added separately to the -P compartment, and the seedlings were sampled after 9 d. JA and ABA were dissolved in ethanol, and DIECA, FLD and sucrose were dissolved in pure water. Accordingly, the mock controls for the JA and ABA treated experiment contained ethanol, and those for the DIECA, FLD and sucrose treatments were pure water.

Root morphology and tissue Pi content assay

Seedlings grown on the plates were photographed with a digital camera (NIKON D750). The length of 1˚LR and 2˚LR, 2˚LR number and total 2˚LR length were measured using ImageJ software. The number of 2˚LRs (including LR and LR primordial; VII and VIII stages) of the seedlings was counted under a stereomicroscope (Olympus SZ61) (Péret *et al.* 2009).

The tissue Pi concentration was measured using the method described by Wang *et al.* (2012), with some modification. Briefly, 50 mg of fresh tissue was homogenized with 50 µL of 5 M H_2SO_4 and 950 µL H_2O. The homogenate was centrifuged at 10000 g for 10 min at 4 °C. The supernatant was collected and diluted to an appropriate concentration. The diluted supernatant was mixed with a malachite green reagent in 3:1 ratio and analysed after 30 min. The absorption values for the solution at 650 nm were determined using a Multifunctional Enzyme Marker (TECAN infinite M200).

Determination of H_2O_2, O_2^-, POD, SOD, soluble sugars, and sucrose

For analyses of H_2O_2, and O_2^- content, peroxidase (POD) and superoxide dismutase (SOD) activities, and soluble sugars and sucrose content, 0.1 g fresh weight root samples were homogenized in 2 mL cold extraction buffer (0.1 M phosphate buffer, pH 7.0). After centrifugation for 10 min at 8000 rpm, the supernatants were used for measurements of the parameters using appropriate assay kits (COMINBO, Suzhou, China (www.cominbio.com)) according to the manufacturer's instructions as described previously (Anwar *et al*., 2018; Chen *et al*., 2019). H_2O_2, O_2^-, soluble sugars, sucrose, POD and SOD were expressed on a fresh weight basis.

Histochemical detection of H_2O_2, O_2^- and callose

H_2O_2 was detected in roots using the DAB (3,3-diaminobenzidine, Sigma-Aldrich) staining method as described previously (Vanacker *et al.*, 2000). The staining solution contained 1 mg/mL DAB in a 10 mM sodium phosphate buffer (pH 7.0) with Tween 20 (0.05% v/v). Roots were incubated in the staining solution at room temperature for 1 h. The root tips of 1˚LR were then visualized and imaged with a stereomicroscope (Olympus SZ61) equipped with a digital camera (Olympus DP73) after rinsing five times in medium solution. Generation of O_2^- in roots was detected by dihydroethidium

(DHE, Invitrogen) staining according to the method described by Yamamoto *et al.* (2002). Roots were incubated with liquid MS medium for 2 h, then loaded with 10 μM DHE for 20 min. After being washed five times with the MS solution, the root tips of 1˚LR were imaged under a confocal microscope (Olympus FV 1000; excitation 543 nm, emission 600–675 nm for DHE). For callose staining, roots were treated for 1.5 h with 0.1 % (w/v) aniline blue (AppliChem) in 100 mM Na-phosphate buffer (pH 7.2) according to the method described by Müller *et al.* (2015). The relative staining/fluorescence intensities of R++ were set as 100%, and the fluorescence intensities of other roots were calculated as the percentage of that for R++ as per He *et al.* (2012). Data are presented as the mean value of at least 20 roots.

Trypan blue staining

Roots of seedlings were incubated in 0.4% trypan blue staining solution at room temperature for 3 min, and then transferred to PBS (phosphate buffer saline) for washing, kept in distilled water and obserrved under a stereomicroscope (Olympus SZ61).

Quantification of callose content in roots

1,3-β-D-glucan (callose) content of roots was quantified using the method described by Santos *et al.* (2005). Briefly, 0.2 g fresh weight root samples were placed in micro centrifuge tubes containing 95 % ethanol for at least 1 h. The alcohol was subsequently decanted and 200 μL of 1 M NaOH was added into the tubes. The samples were ground and then placed in a water bath at 80 °C for 15 min to solubilize callose and then centrifuged at 15000 g for 4 min. The supernatant (400 μL) was incubated with 800 μL 0.1 % aniline blue, 420 μL 1 M HCl, and 1180 μL glycine-NaOH buffer (pH 9.5) for 20 min at 50°C and then for 30 min at the room temperature. Callose content was estimated using a Multifunctional Enzyme Marker (TECAN infinite M200) with excitation at 398

nm and emission at 495 nm. Pachyman (Calbiochem, LaJolla, CA, USA) was used as an external standard and callose content was expressed as mg Pachyman equivalent (PE) per g root fresh weight.

Determination of MDA content

The MDA content was measured according to the modified thiobarbituric acid (TBA) method described by Wang *et al.* (2009). Approximately 0.1 g fresh weight root samples were homogenized in 750 µL of 5 % tri chloroacetic acid (TCA) and centrifuged at 3000 rpm for 10 min. The supernatant was mixed with 200 µL of 5 % TCA containing 0.67 % TBA. The mixture was heated to 100 °C for 30 min and cooled on ice. After centrifugation at 12000 rpm for 5 min, the absorbance of the supernatant at 532 nm was recorded. Non-specific absorbance at 600 nm was measured and subtracted from the readings recorded at 532 nm. Concentration of malonaldehyde (MDA) was calculated using its extinction co-efficient, 155 mM^{-1} cm^{-1}.

Extraction and analysis of endogenous plant hormones

Extraction and analysis of endogenous plant hormones were conducted according to the method described by Liu *et al.* (2012). The supernatant was gathered and injected into UFLC-ESI-MS/MS (ultrafast liquid chromatography-electrospray ionization/tandem-mass spectrometry system. Five biological replicates were analysed for each treatment. The standard of JA was purchased from Sigma-Aldrich (St. Louis, MO, USA), and the standards for ABA and JA-Ile were purchased from OlChemIm (OlChemIm, Olomouc, Czech Republic). The internal standards were $^{2}H_{6}$ABA (Olchemin) for ABA, 10-dihydro-JA (DHJA; Olchemin) for JA and JA-Ile. All these standards and internal standards were kindly provided by Dr. Hongbo Liu from the National Key Laboratory of Crop Genetic Improvement, Huazhong Agricultural University.

RNA-seq and analysis

Four biological replicates from each treatment were used for transcriptome analyses. Each biological replicate was a composite sample, which had 20 roots from independent plates. Total RNA was extracted using a RNAiso Plus kit (TaKaRa, Dalian, China) according to the manufacturer's instructions. The integrity of the RNA was checked by electrophoresis on a 1% agarose gel and spectrophotometrically with a NanoDrop^{TM}2000 UV-vis Spectrophotometer (Thermo Scientific, Waltham, MA). The transcriptome sequencing was performed by Novogene (Beijing, China). The library construction was carried out according to the Illumina standard instructions and was sequenced on the Illumina HiSeq 2000 platform. To obtain high-quality clean reads, the adaptor reads, unknown nucleotides, low-quality reads were removed from the raw reads. The clean reads were then aligned to the ZS11 genome (Sun *et al.*, 2017; Song *et al.*, 2020) using Bowtie2 and HISAT2 software. The Fragments Per Kilobase of transcript per Million mapped reads (FPKM) method was used to calculate the expression levels of genes. Differential expression of the genes between treatments was then analysed using the DESeq R package (http://www.bioconductor.org/packages/release/bioc/html/DESeq.html). Genes with fold change $|\log_2 FC| > 1$ and $P < 0.05$ were deemed to be significantly differentially expressed genes (DEGs). To determine the biological significance of the DEGs, transcripts in all samples were searched by BLASTN with an $E < 10^{-5}$ against the TAIR database (http://www.*Arabidopsis*.org/ Blast/index.jsp). Then, the unigenes (AGI identifiers) were used to annotate these DEGs. Annotated genes were attributed functions using the GO database (http://geneontology.org/) using the Blast2Go program and to biological pathways using the KEGG database (http://www.genome.jp/kegg). GO terms and biological pathways with a $P < 0.05$ were deemed to be significantly enriched in DEGs.

Real-time quantitative reverse transcription PCR (RT-qPCR) analysis

To assay the relative expression levels, RT-qPCR analysis was performed with the total RNA extracted as described above. The total RNA was used as templates (1 μg each) for the first-strand cDNA synthesis with a HiFiScript cDNA Synthesis Kit (CWBIO, Beijing, China) according to the manufacturer's instructions. RT-qPCR analysis with gene-specific primers (Table S2) was conducted on a CFX96^{TM} Real-time PCR Detection System (Bio-Rad, Hercules, CA, USA) using Hieff qPCR SYBR Green Master Mix (Yeasen, Shanghai, China) based on the manufacturer's protocol. *Tubulin* and *EF1α* were used as internal control gene to normalize samples, and relative gene expression levels were measured using the $2^{-\Delta\Delta CT}$ method. Three biological replicates were used for each sample.

In order to check the early transcriptional responses of *B. napus* in split-root treatments, the expression levels of some representative genes (ABA, JA, sugar and ROS related genes) were examined by RT-qPCR.

Statistical analysis

Statistical analysis of the data was conducted using one-way analysis of variance (ANOVA) or t-test in SPSS (IBM, New York, NY) and Microsoft Office Excel, assuming $P < 0.05$ as a significance threshold.

Results

Heterogeneous availability of Pi significantly alters the RSA of B. napus seedlings

The shoot fresh weight of the plants grown with a heterogenous Pi supply (S+-) was similar to that of the plants with homogenous Pi availability (S++), but both were significantly larger than that of Pi-starved plants (S--) (Figure 1b-c). Root

fresh weights followed the series R+ > R++ > R-- > R- (Figure 1b, c). Furthermore, the Pi concentration in S+- was 25% lower than that in S++, but 100% higher than that in S-- (Figure 1d). The Pi concentration in R-- was only 25% of that in R++, whereas the Pi concentration in the R+ was similar to that of R++. The Pi concentration in R- was higher than that in R--, but lower than that in R+ (Figure 1d).

The plants grown with a homogenous low Pi supply had shorter 1˚LR, but more 2˚LR than those grown with a homogenous high Pi supply (Figure 1b, e-g). Root morphology of the plants grown with heterogeneous Pi availability was significantly different to the roots of the plants grown with homogenous Pi availability (Figure 1b). The elongation rate of 1˚LR of R+ was similar to R++, but that of R- was significantly greater than R-- (Figure 1e, f). Also, the development of 2˚LR (Figure 1g, h) and their length (Figure 1i, j) were greatest in R+ and least in R-. Collectively, these data suggest that LR growth of *B. napus* seedlings is mainly regulated by systemic signalling.

Transcriptomic analysis of genes locally or systemically regulated by Pi starvation

In order to understand the molecular mechanisms regulating the morphological and physiological responses of *B. napus* seedlings to heterogeneous Pi availability, RNA-seq analysis was performed, and pairwise comparisons of gene expression levels among treatments conducted. Following quality checks and exclusion of null reads, a total of 108.7 Gb (with a GC content of 46.31 and a Q30 of 89.48%) of paired-end clean reads were generated across 16 root samples (Table S1). These clean reads were mapped to the *B. napus* ZS11 reference genome (Sun *et al.*, 2017; Song *et al.*, 2020).

Transcriptomic differences in the R++ vs. R-- comparison were the largest among all the pairwise comparisons with a total of 4793 differentially expressed genes (DEGs), 2935 being up-regulated and 1858 down-regulated

(Figure 2a). The comparison with the smallest difference in DEGs was R- vs. R+, with only 306 DEGs identified, 150 being up-regulated and 156 down-regulated. In addition, a total of 4080 and 1653 DEGs were identified in R-- vs. R- and R++ vs. R+, respectively (Figure 2a). The transcriptome data were validated by quantitative reverse transcription-PCR (RT-qPCR). The expression patterns of the 14 randomly selected genes assayed by RT-qPCR were largely in agreement with those assayed by RNA-seq, as reflected by a high correlation coefficient (R^2 = 0.88) between the two methods (Figure S1).

The DEGs were divided into two categories according to the relative expression levels of genes between R++ and R--. The genes whose expression levels in R-- were significantly higher and lower than that in R++ were defined as Pi-starvation-induced genes and Pi-starvation-repressed genes, respectively. These DEGs were then classified according to their expression levels in R+ or R-: (i) locally regulated genes were designated as transcripts with a similar expression level between R++ and R+ or R-- and R- (Figure 2b, c), whereas (ii) transcripts with significantly different expression levels in R+ and R- versus their respective controls (R++ and R--) were termed systemically regulated genes (Figure 2 d-g). We identified 894 locally induced and 971 locally repressed genes by Pi starvation, respectively. These genes were only regulated by the Pi levels in the adjacent medium and the transcription levels of the up-regulated or down-regulated genes between R+ and R++, and between R- and R-- were similar (Figure 2b, c). The systemically regulated genes were divided into four groups based on the transcription levels of R+ and R-, reflecting a hierarchical change in the response to Pi starvation. Two groups are based on the systemic repression of genes in R- or R+ when compared with R-- or R++ but where the transcription level displayed no significant difference between R++ and R+ or R-- and R-, respectively (Figure 2d and f). A total of 1778 and 328 genes were identified in these two groups, they were either systemically induced or repressed by Pi starvation (Figure 2d,

f). Among these two groups, the induced genes in R- (Figure 2d) and the repressed genes in R+ (Figure 2f) were modulated systemically, and their transcriptional levels were lower than that in R-- and R++, respectively. In the other two groups, the transcription level of genes in R+ (Figure 2e) and R- (Figure 2g) were both modulated systemically and they were between the transcription level of R++ and R--. The number of genes in these two groups were 52 and 51, respectively. Taken together, the number of systemically regulated genes was more than that of locally regulated genes, and almost half (45%) the Pi starvation-regulated genes were systemically induced, indicating systemically induced genes may play vital roles in response to Pi starvation.

The P1BS element is central to the responses of plants to Pi starvation (Sobkowiak *et al.*, 2012). The proportion of genes containing a putative P1BS element in their promoter in different groups of genes was investigated (Figure 2h). Compared to locally regulated genes and systemically repressed genes, systemically induced genes had a higher proportion of genes containing P1BS in their promoter region (Figure 2h). This supports the notion that systemically induced genes are central to the Pi-deficiency signal transduction pathway.

Functions of genes regulated locally and systemically by Pi starvation

Genes locally induced and repressed by Pi starvation were both associated with hormone-related responses, including biosynthesis, transport and response to ethylene (induced: *ERF*, *EDF*, *EFE*), jasmonic acid (induced: *JAZ10*), auxin (induced: *IAA7*, *IAA29*, *PIN*; repressed: SAUR-like auxin-responsive protein family, *IAA16*), abscisic acid (induced: *ZF2*; repressed: BURP domain-containing protein, *PP2C5*), gibberellin (repressed: gibberellin-regulated family protein, gibberellin-oxidase) and involved in the homeostasis of metals such as iron, zinc, copper and potassium, etc. (induced: *FER3*, *YSL2*, *ZIP*, *CCH*, etc.; repressed: *VIT*, *COPT2*, *AKT3*, etc.). In addition, a large number of genes encoded transcription factors (*WRKY*, *NAC*, *MYB*,

bHLH, etc.). A Pi transporter (*PHT3;1*) and two phosphate transporter traffic facilitator1 (*PHF1*) genes were locally induced and transporters for other substances (*MFS*, *AAP*, *MATE*, *NIP*, etc.) were locally induced or repressed. In addition, 14 locally-induced genes were associated with stress-related responses, which encoded cytochrome P450, and disease resistance and response to stress proteins, 25 locally-repressed genes were implicated in cell wall synthesis (expansin, *CEL3*, *CSLA7*), cell activity and growth (*LRR*, *LRR-RK*, etc.), lateral root primordium (lateral root primordium (LRP) protein-related) and root hair growth (*RSL4*), and Pi recycling (HAD superfamily, subfamily IIIB acid phosphatase and *PAP15*) (Figure 3a and Table 1).

Genes systemically-induced or repressed by Pi starvation were also associated with hormone-related responses, including biosynthesis, transport and response to auxin (induced and repressed: auxin-responsive family protein, etc.), jasmonic acid (induced: JAZ, *HCHIB*; repressed: *SQE3*), abscisic acid (induced: *NCED3*, *HAI2*, *RCAR1*, *PP2C5*, *PLP4*, *PDR*; repressed: *ALDH3I1*, *AAO2*), gibberellin (induced: gibberellin-regulated family protein), ethylene (induced: *ERF*) and salicylic acid (repressed: UDP-glucosyltransferase 75B1). In addition, 24 systemically induced genes involved in Pi recovery, including *PHT1;3, PHT1;4, PHT1;5, PHT1;8, PHT1;9, PHT4;2 and PHF1*, and two systemically repressed genes encoded low-affinity Pi transporters *PHT2;1*. In addition to these Pi transporters, systemically regulated genes were also involved in regulating the homeostasis of other nutrients. For example, transporters of sulphur (*LSU2*, *SULTR3*, *AST91*), nitrogen (*NRT1.7*, *NAXT1*, nitrate transmembrane transporters), potassium (*KUP9*, *KAT1*, *KAT2*), zinc (*ZIP4, ZIP5*), copper (*COPT1*), and iron (*VIT*) were systemically induced, and those of iron (*FRO2*, *FD3*, *IRT1*), nitrogen (*NRT1.1*, *NRT1.7*, *NIA1*, *TIP2;3, AMT1;5*), calcium (*CAX1*, *CAX7*), boron (*NIP6;1*) and sulfur (*SULTR1;2*) were systemically repressed. Similarly, a large number of

transcription factors were systemically induced (120) and repressed (20) by Pi starvation, such as *WRKY*, *NAC*, *MYB*, *bHLH*, *bZIP*, *WOX*, etc. In addition, many genes related to Pi recycling, such as acid phosphates (*PAP*) and enzymes involved in phospholipid remobilization, galacto- or sulfo- lipid synthesis and nucleases (*SQD1*, *SQD2*, *MGDC*, *PLC*, *NPC4*, *PS2* and *BFN1*) were induced. Notably, we found that 7 SPX genes (*SPX1*, *SPX2* and *SPX3*) and one *PHO1;H1* gene associated with Pi signalling and sensing were also induced. Several (28) genes related to metal binding, such as zinc binding (13; *STH*, *BCA*, etc.) and iron binding (15; 2OG and Fe(II)-dependent oxygenase superfamily protein, cytochrome P450, etc.), were systemically repressed by Pi starvation (Figure 3b and Table S3).

GO annotation and KEGG pathway analysis of the DEGs systemically-induced by Pi-starvation

The expression of 96% of 1830 systemically- induced genes were strongly repressed in R- compared to R-- (Figure 4a, b). These genes may play significant roles in the systemic response to Pi starvation. Among the top 20 significantly enriched biological process, many systemically-induced DEGs were enriched in five GO terms associated with hormones, including “response to hormone”, “response to abscisic acid”, “response to jasmonic acid”, “jasmonic acid mediated signalling pathway”, “abscisic acid-activated signalling pathway” and four GO terms related to redox status regulation, including “response to oxygen-containing compound”, “oxidation-reduction process”, “response to oxidative stress” and “regulation of reactive oxygen species metabolic process” (Figure 4c). KEGG enrichment analysis of systemically- induced DEGs showed that the greater number of enriched genes were observed in five pathways, “phenylpropaniod biosynthesis”, “glycerolipid metabolism”, “cutin, suberin and wax biosynthesis”, “starch and sucrose metabolism”, and “plant hormone signal transduction” (Figure 4d).

ABA and JA signalling pathways are involved in Pi starvation responses

Six hormone-related GO terms associated with ABA and JA signalling pathways were significantly enriched in genes induced systemically by Pi starvation (Figure 4c). The expression patterns of 41 genes in the ABA-activated signalling pathway GO term and 43 genes in the JA-mediated signalling pathway GO term were analysed in detail (Figure 5a; Table S4). A total of 18 genes were present in both signalling pathways, such as *jasmonate-zim-domain protein* (*JAZ*), *myb-domain protein* (*MYB*) and *calcineurin B-like protein* (*CBL*), implying crosstalk between the ABA and JA pathways in the systemic regulation of Pi starvation responses. Twenty-three genes associated with the ABA-activated signalling pathway GO term showed higher expression in R-- than in R++, R+ and R- (Figure 5a and Table S4). In addition, the expression of *nine-cis-epoxycarotenoid dioxygenase 3* (*NCED3*, *BnA01g0036580.1*) that codes a key rate-limiting enzyme in ABA biosynthesis (Zhang *et al.*, 2009; Sun *et al.*, 2012) was highest in R-- roots (Table S4), and so was their ABA concentration (Figure 5b, c).

The expression of 25 genes associated with the JA-mediated signalling pathway was highest in R-- plants (Figure 5a; Table S4). JA and its biologically active metabolite JA-isoleucine (JA-Ile) are lipid-derived compounds that are synthesized from α-linolenic acid by one of seven branches of the lipoxygenase (LOX) pathways (Feussner and Wasternack, 2002; Fonseca *et al.*, 2009). Lipoxygenases (LOXs) catalyse the oxygenation of fatty acids to their hydroperoxyl derivatives, which are required for JA biosynthesis (Schaller, 2001). In our study, the transcript levels of two *LOXs* were highest in R-- plants (Table S4); this was reflected in tissue JA and JA-Ile concentrations (Figure 5d-g) indicating that Pi starvation may trigger changes in root JA levels, which act as part of the systemic signalling mechanism.

Functional assays demonstrated that shoot growth of plants grown in the

split-root system with heterogeneous Pi availability was inhibited by exogeneous JA but promoted by a JA biosynthesis inhibitor (Figure 6a, b), and that R+ and R- roots responded differently to JA application (Figure 6a, c). When R- was treated with exogeneous JA, 1˚LR elongation of R+ and R- were both inhibited (Figure 6d), and 2˚LR number and total 2˚LR length of R- were significantly decreased. However, 2˚LR density, 2˚LR average length and total 2˚LR length of R+ roots were significantly increased (Figure 6f-h). Opposite effects were reported for roots treated with a JA biosynthesis inhibitor Figure 6d-h). Taken together, these data indicate a functional role of JA in the systemic Pi starvation response (PSR).

ABA significantly inhibited R- growth (Figure 7a-c) and 2˚LR growth (Figure 7d-h), but increased 2˚LR density of R+ (Figure 7a, f). Reduction of ABA concentration by its biosynthesis inhibitor FLD significantly increased shoot fresh weight (Figure 7a-b), promoted 1˚LR elongation of R-, but decreased 2˚LR number, 2˚LR density, average 2˚LR length and total 2˚LR length of R+ compared to untreated plants (Figure 7d-h). These data indicate that ABA enhances systemic PSR by inhibiting growth of R- and promoting 2˚LR density of R+.

Genes for sugar metabolism are involved in systemic regulation of Pi starvation responses

The pathway of starch and sucrose metabolism was enriched in DEGs systemically induced or repressed by Pi starvation, implying that this pathway may be critical for systemic regulation of PSR. Seventeen DEGs in the ‘Starch and sucrose metabolism’ pathway were analysed in detail. Seven DEGs were associated with sucrose synthesis, and seven other DEGs were associated with fructose or glucose synthesis (Figure 8a). The expression of these genes was highest in R-- roots (Figure 8a), as were the concentrations of soluble sugars and sucrose (Figure 8b-e). These results suggest that the synthesis of

sugars in the shoot and their transport to the root were regulated systemically by Pi starvation, and that sugars might be a key component of the systemic Pi-starvation regulation of RSA.

Sucrose can act as a systemic signal, being transported from the shoot to root (Hammond and White, 2011; Ham *et al*., 2018). In order to confirm the role of sucrose in regulating RSA under heterogenous Pi-starvation conditions, R- was treated with sucrose. Compared to untreated plants, sucrose did not increase shoot fresh weight, but significantly increased fresh weight of R+ (Figure 9a-c). In the roots of R-, sucrose significantly inhibited 1˚LR elongation and 2˚LR number of R- (Figure 9d, e), but had no effect on 2˚LR density, 2˚LR average length and total 2˚LR length (Figure 9f-h). In roots of R+, sucrose significantly increased 2˚LR average length and total 2˚LR length of R+ (Figure 9g, h), but did not alter 1˚LR length, 2˚LR number or 2˚LR density (Figure 9d-f). These findings indicate that sucrose enhances systemic PSR by inhibiting 1˚LR growth and 2˚LR number of R- and increasing the average length of 2˚LR and total 2˚LR length of R+ roots.

Oxidative stress-related genes are involved in protecting the plant from Pi-starvation stress

In the biological process GO categories, four terms in antioxidant processes and one term in callose deposition were enriched in DEGs (Figure 4a), suggesting that ROS and callose accumulation may be involved in protecting the plant from stresses associated with Pi-starvation. The transcript levels of 28 genes enriched in the response to oxidative stress GO term were highest in R-- plants (Figure 10a) including those encoding peroxidase superfamily proteins (POD) and three genes encoding copper/zinc superoxide dismutases (Cu/Zn-SOD) responsible for ROS scavenging (Choudhury *et al.*, 2016). The activities of POD and SOD were greatest in R-- plants (Figure 10d, e). ROS induces callose deposition in the cell wall of the root tip, which plays an

important role in root development (Dunand *et al.*, 2006; Benitez-Alfonso *et al.*, 2011). The concentrations of two major ROS, hydrogen peroxide (H_2O_2) and superoxide radical (O^{2-}), and callose deposition, in plant roots were observed by DAB, DHE and aniline blue staining, respectively. The histochemical staining with DAB and DHE showed the strongest signals in the root tips of R-- plants (Figure 10b, c), as did the fluorescence intensity of aniline blue. Consistent with these findings was *in situ* accumulation of ROS (H_2O_2 and O_2^-) and callose in root tips (Figure 10f-h). ROS-induced lipid peroxidation assessed by malondialdehyde (MDA) content showed markedly higher MDA content in R-- compared with R++, R+ and R- (Figure 10i). In general, the accumulation of ROS and ROS-induced callose deposition and lipid peroxidation were all more pronounced in R-- than in R++, R+ and R- (Figure 10a~i).

Discussion

Changes in RSA in response to localised Pi availability

Phosphate availability in the soil often shows a heterogeneous distribution because of its low mobility. To overcome low Pi availability, plants have evolved a wide array of mechanisms aimed at modifying RSA to increase root proliferation in Pi-enriched patches (Sun et al., 2018; Wang et al., 2019). Our previous studies showed that 625 µM phosphate in the agar medium is an optimum P supply (Shi *et al.*, 2013), as SDW and RDW were less at both low/no P conditions as well as at 1250 µM phosphate than at 625 µM phosphate. Thus, in the current study, 625 µM phosphate was used as the control (+P, optimum supply).

In this study, heterogeneous Pi availability (+P/-P) did not affect shoot growth (shoot fresh weight) (Figure 1b-d). At the same time, heterogeneous Pi availability increased root fresh weight of R+ but decreased that of R- (Figure

1c), illustrating the preferential partitioning of biomass to the place with greater Pi availability. Pi concentration in R+ was higher than that in R-, and the density and total length of 2˚LR in R+ were also greater than those in R- (Figure 1d, h, j), which allows plants to compensate for restricted Pi acquisition by other parts of the root system. Compared with R++ and R--, Pi distribution in R+ and R- also suggesting relatively high mobility of Pi from R+ to R- via the shoot. Previous studies have also shown that greater root proliferation contributed to Pi uptake capacity in Pi-rich patches and, thereby, maintained biomass production (Shen *et al.*, 2005; Funakoshi *et al.*, 2015; Wang *et al.*, 2019). These data suggest a key strategy to maintain high yields with low fertilizer input by local or banded application of phosphorus fertilizers.

Pi deficiency inhibits primary root elongation and increases lateral root length and density (López-Bucio *et al.*, 2002; Sánchez-Calderón *et al.*, 2005; Richardson and Simpson, 2011; Trachsel *et al.*, 2011; Ruiz-Herrera *et al.*, 2015). In this study, the 1˚LR length was inhibited while 2˚LR length and density were increased in -P/-P medium (Figure 1b, e-j), implying that 1˚LR may function similarly to the primary root after the primary root is removed. 1˚LR growth was mainly determined by the Pi concentration in the growth medium whether plants were grown with a heterogeneous P supply or at homogeneous Pi supply (with or without Pi) (Figure 1 b-c, e-f). In addition, this pattern also matched the Pi concentration in roots (Figure 1 d), indicating that 1˚LR elongation might be modulated not only by the external Pi concentration in the growth medium, but by the intracellular Pi concentration in roots. 1˚LR length of R- was longer than that of R-- (Figure 1b, f), which differed from that observed in *Arabidopsis* (Thibaud *et al.*, 2010). Heterogeneous Pi availability markedly decreased 2˚LR density of R- and promoted 2˚LR initiation and elongation of R+ (Figure 1g-j), which was indicative of systemic P-demand signals from R- and systemic P-supply signals from R+. To our knowledge, no study reported that 2˚LR number, density, average length and total length of R-

decreased as compared with R-- in Arabidopsis (Thibaud *et al.*, 2010; Oldroyd and Leyser, 2020) and other crops (Wang *et al.*, 2019). RSA responses of *B. napus* and *Arabidopsis* to heterogeneous Pi availability are not completely consistent.

The seed of *B. napus* is very small, and the seed P reserves probably lasted only 5-6 days in the experiments reported here, judged by the fact that cotyledons became yellow and purple after that time in plants lacking a P supply. In this study, seedlings of *B. napus* were first grown with sufficient Pi for 6 d, and then transferred to the spilt-root system with different Pi availabilities for 9 d (Figure 1a). Both 1˚LR and 2˚LR growth showed significant differences among treatments after 9 d of treatment (Figure 1e-j). It is, therefore, likely that it was the Pi in the medium, rather than the P in the seed, that affected the responses of *B. napus* to Pi availability in our experiments.

Locally and systemically regulated transcriptional responses to Pi starvation

Transcriptional changes of gene expression play pivotal roles in the modulation of physiological and biological processes (Zhu, 2016). The pairwise comparison of R++ vs. R-- had the greatest number of DEGs and the R+ vs. R- pairwise comparison had the least number of DEGs, suggesting that gene expression in roots with heterogeneous Pi availability was responding mainly to Pi starvation (Figure 2a). These DEGs were divided into different groups according to a previous study of *Arabidopsis*; but it was recognised that some of systemically induced and repressed genes might also be controlled by local Pi availability (Figure 2d and 2f). This implies the co-regulation of genes by local and systemic signals in response to Pi starvation. Changes in root morphology with heterogeneous Pi availability were mainly regulated systemically (Figure 1b-j). This was consistent with the observation that more genes were regulated systemically than were regulated locally (Figure 2b-g).

627 Furthermore, 1˚LR growth was consistent with the expression of systemically-
628 induced genes by Pi starvation (Figure 1f; Figure 2d).
629 Consistent with previous observations (Thibaud *et al.*, 2010), genes
630 associated with Pi homeostasis (Pi recovery, Pi recycling and Pi sensing) were
631 generally systemically induced by Pi starvation (Figure 3b), while genes
632 associated with metal binding were systemically repressed (Figure 3b),
633 implying different strategies for dealing with Pi and metal availability (e.g.,
634 systemic vs local response). In *Arabidopsis*, many genes related to hormonal
635 metabolism were induced locally by Pi starvation (Thibaud *et al.*, 2010).
636 However, our findings revealed that genes associated with hormone-related
637 responses were regulated both locally and systemically by Pi starvation in *B.*
638 *napus* (Figure 3). This is consistent with earlier reports that hormones are
639 implicated in both local and systemic responses to Pi starvation, and that Pi
640 availability can alter hormone biosynthesis, transport and sensitivity (Rubio *et*
641 *al.*, 2009; Chiou *et al.*, 2011; Ham *et al.*, 2018).
642 Pi-starvation-induced genes often contain the P1BS sequence in their
643 promoters (Bustos *et al.*, 2010). In Arabidopsis, systemically-induced genes
644 were enriched in the P1BS sequence compared to the entire genome (Thibaud
645 *et al.*, 2010). In our study, 83% of the genes induced systemically by Pi
646 starvation contained the P1BS binding site (Figure 2d and h), and 99% of
647 these genes were specifically, systemically-induced DEGs (Figure 4a). This
648 indicates that BnPHR1 is a major component of the Pi signal transduction
649 pathway regulating systemically-induced genes in the Pi starvation response
650 of *B. napus*.
651 A large number of genes modulated by Pi starvation were regulated locally in
652 *Arabidopsis thaliana* (Thibaud *et al.*, 2010) after 2 days of growth in a split-root
653 system. Our study on *B. napus* involved older plants, and longer (9 d) Pi
654 starvation; and most DEGs were regulated systemically (Figure 2b-g). The
655 transcriptional responses of root to Pi starvation between *B. napus* and

Arabidopsis are different. A plausible explanation for the contrasting observations of Thibaud *et al.* (2010) and the present paper could be that transcriptional responses to short-term Pi starvation are primarily mediated by external Pi availability, while the response to long-term Pi starvation is mainly mediated by intercellular Pi concentrations. However, the expression patterns of genes related to hormone (JA and ABA) signalling, sugar metabolism and ROS following short-term (2 d) exposure to heterogeneous Pi availability were similar to those following 9 d exposure of *B. napus* to heterogeneous Pi supply (Figure S2).

JA and ABA are involved in systemic responses to Pi starvation

Hormones are important components of Pi signalling regulatory networks (Ha and Tran, 2014; Puga *et al.*, 2017). Hormone-related genes in *Arabidopsis* were only locally regulated by Pi starvation (Thibaud *et al.*, 2010), while hormone-related genes in *B. napus* were both locally regulated and systematically regulated by Pi starvation (Figure 3). A large number of DEGs induced systemically by Pi starvation were significantly enriched in the GO terms of the ABA and JA-mediated signalling pathways (Figure 4c and 5a), suggesting that ABA and JA are both involved in systemic responses of *B. napus* to Pi starvation (Figure 4d).

Previous studies have indicated that JA induction and Pi starvation share some common phenotypes, including growth reduction and anthocyanin accumulation, implying a potential role of JA in PSR (Shan *et al.*, 2009; Yang *et al.*, 2012). It was also suggested that JA may play an important role in the inhibition of PR growth triggered by Pi-starvation (Chacón-López *et al.*, 2011). In our study, the genes associated with JA signalling were systemically induced by Pi starvation (Figure 5a; Table S4). Among them, JAZs are key components in the JA signal transduction pathway and are rapidly induced in response to Pi deficiency (Mosblech *et al.*, 2011; Khan *et al.*, 2016). The

transcript levels of two *BnLOXs* (*BnA03g0128810.1* and *BnC02g0496310.1*), encoding an important enzyme in the JA and JA-Ile biosynthetic pathway (Schaller, 2001), were significantly higher in R-- roots than in R++, R+ and R- roots (Figure 5a and Table S4), and the JA and JA-Ile concentrations in shoots and roots of plants in the -P/-P treatment were significantly higher than those in the -P/+P and +P/+P treatments (Figure 5d-g). Therefore, compared to S-- and R--, less accumulation of JA and JA-Ile in S+- and R- may be a result of higher Pi concentration in S+- and R- (Khan *et al.* 2016).

Addition of JA to -P medium appeared to enhance the Pi-starvation signal from R- in the split-root system that inhibited 1˚LR and 2˚LR growth of R- and increased 2˚LR density, 2˚LR average length and total 2˚LR length of R+ (Figure 6a, d-h). In contrast, inhibition of JA biosynthesis appeared to reduce the Pi-starvation signal from R- (Figure 6d-h). Taken together, these findings provide strong evidence for the role of JA signalling in systemic regulation of RSA in plants grown with heterogeneous Pi availability.

The transcriptomic analysis of *Arabidopsis* subjected to different hormone treatments and Pi starvation showed that among these hormones, ABA displayed the most interaction with Pi starvation (Woo *et al.*, 2012). We also found that the genes associated with ABA signalling, including *PYL10*, *RCAR1*, *PP2C*, *NCED3*, were systemically induced by Pi starvation (Figure 5a and Table S4). *PYL10* and *RCAR1* (ABA receptors) and their downstream *PP2Cs* are key components in ABA signal transduction (Ma *et al.*, 2009; Hao *et al.*, 2011). Furthermore, the expression of *NCED3* (a key ABA biosynthetic enzyme) was correlated with ABA concentrations in roots (Figure S1 and Figure 5c). Previous studies have similarly reported that greater expression of *NCED3* increases ABA biosynthesis (Takahashi *et al.*, 2018). R-- accumulated more ABA than R++ (Figure 5c), and the inhibition of ABA biosynthesis in R- might be explained by greater Pi concentrations in R- than R-- roots (Figure 1d) or a systemic signal from R+.

714 Exogeneous ABA apparently enhanced the Pi-starvation signal from R- roots
715 and systemic PSR by inhibiting 1˚LR elongation and 2˚LR growth of R- and
716 promoting 2˚LR density and root hair growth of R+ (Figure 7a, d-f). Inhibition of
717 ABA biosynthesis significantly decreased the Pi-starvation signal from R- roots
718 and attenuated the systemic PSR by increasing 1˚LR length of R- and
719 decreasing 2˚LR growth and root hair growth of R+ (Figure 7a, d-f). This
720 indicates that ABA may be also an important signal involved in the long-term
721 systemic responses to Pi starvation.
722
723 ***Sugar metabolism in the systemic responses to Pi starvation***
724 Sucrose and starch metabolism have been reported previously to be involved
725 in PSR, and sucrose has been proposed as an important systemic signal that
726 participates in the regulation of RSA in plants lacking Pi (Hermans *et al.*, 2006;
727 Jain *et al.*, 2007; Hammond and White, 2008; Müller *et al.*, 2007; Hammond
728 and White, 2011; Chiou *et al.*, 2011; Pant *et al.*, 2015). The addition of sucrose
729 to Pi-starved plants enhances PSR gene expression and modifies root growth
730 (Liu *et al.*, 2005; Lei *et al.*, 2011). In this study, many genes related to sugar
731 metabolism were systemically induced by Pi starvation (Figure 8a). These
732 genes included *SPS*, *SPP, FRUCT and BGLU* that encode enzymes involved
733 in sucrose, glucose and fructose metabolism (Fernández *et al.*, 2004; Chen *et*
734 *al.*, 2005; Haigler *et al.*, 2007; Zhao *et al.*, 2013). The expression of these
735 genes was significantly higher in R-- than in R++, R+ and R- roots (Figure 8a).
736 Also, soluble sugars and sucrose concentrations were significantly higher in
737 S-- than in S++ and S+, and in R-- than in R++, R+ and R- (Figure 8b-e). Pi
738 starvation promotes sugar accumulation in the shoot and also its translocation
739 from the shoot (source) to the root (sink), which suggests that it might act as a
740 systemic Pi signal reporting shoot P-demand to the root and promoting root
741 growth (Ciereszko *et al.*, 2005; Dasgupta *et al.*, 2014). In our study, sugar
742 concentrations in R- were significantly less than that in R--, but similar to those

743 in R+, suggesting that the P-demand of S+- from R- is lower than that of S--
744 from R-- because of the former received a systemic signal of Pi availability
745 from R+ (Figure 1d and Figure 8c, e). Plants treated with exogeneous sucrose
746 showed greater Pi starvation symptoms and more P-demand in R- than R+ in
747 the split-root (P+/P-) system, and this enhanced systemic PSR by decreasing
748 1˚LR length and 2˚LR number of R- and increasing 2˚LR average length and
749 total 2˚LR length of R+ (Figure 9d-h). Therefore, sugar metabolism is involved
750 in long-term systemic responses to Pi starvation and could potentially be
751 interacting with JA and ABA signalling pathways.
752
753 ***ROS production in Pi-starvation stress***
754 ROS are usually deemed to be toxic and excessive accumulation of ROS
755 leads to inhibition of plant growth and development (Choudhury *et al.*, 2016).
756 ROS concentrations in roots are increased by Pi starvation (Shin *et al.*, 2005).
757 POD and SOD are two key antioxidant enzymes that play a vital role in
758 elimination of H_2O_2 and $\cdot O_2^-$ respectively (Choudhury *et al.*, 2013; Gong *et al.*,
759 2020). Our study indicated that the expression of *POD* and *SOD* genes were
760 systemically induced by Pi starvation (Figure 8a). In agreement with the
761 transcript levels of the genes, POD and SOD activities were also much higher
762 in R-- than in the R++, R+ and R- (Figure 10d, e), suggesting that R-- needs
763 more ROS-scavenging enzymes to detoxify excessive ROS than R++, R+ and
764 R-. This suggestion is supported by the higher accumulation of both H_2O_2
765 and $\cdot O_2^-$ in R-- roots than R++, R+ and R- roots (Figure 10b-c, g-h). These
766 findings agree with previous reports that Pi-starvation increases ROS
767 production and activity of ROS-scavenging enzymes (Shin *et al.,* 2005; Zhang
768 *et al.,* 2020). In addition, there was no significant difference in trypan blue
769 staining among R++, R+ and R-, but staining of R-- was deeper than R++, R+
770 and R-, which indicated that ROS accumulation was caused by Pi-starvation
771 and not by apoptosis (Figure S3). In agreement with the accumulation of ROS

772 in different roots, MDA and callose concentrations in R-- were also higher than
773 those in R++, R+ and R- (Figure 10b-c, f-i). ROS have been reported to
774 accumulate in PR meristem and inhibit PR growth in local responses to Pi
775 starvation (López-Bucio *et al.*, 2002). However, Pi starvation induced ROS
776 accumulation in the elongation zone of young LR and promoted LR growth,
777 while in meristem of older LR they inhibited LR growth (Tyburski *et al.*, 2009).
778 ROS may also act as secondary signals participating in systemic responses to
779 Pi starvation (Chiou *et al.*, 2011). In our study, ROS accumulation in R- was not
780 significantly different to R+ and R++, but 1˚LR length of R- was shorter than R+
781 and R++ (Figure 1f and Figure 10b-c, g-h). This might be attributed to the fact
782 that 1˚LR elongation is mainly regulated by external Pi, which resulted in a
783 slower 1˚LR elongation rate of R- than R+ and R++ immediately after transfer
784 to the treatments (Figure 1e); however, 1˚LR elongation rate of R- began to
785 increase after 4 d (Figure 1e), which could be associated with the decrease in
786 ROS accumulation in R- at this time. Finally, ROS accumulation in R- was
787 similar to that in R++ and R+ after 9 d of treatment, but 1˚LR length of R- was
788 shorter than that of R++ and R+ (Figure 1f and Figure 10b-c, g-h).
789
790 **Conclusions**
791 In this study we analysed the changes of RSA to homogeneous and
792 heterogeneous Pi availability in *B. napus* and found that 2˚LR growth was
793 regulated mainly systemically by Pi starvation. Systemic P-demand (−P)
794 signalling promotes 2˚LR growth of R+ (in blue) and systemic P-supply (+P)
795 signalling inhibit 2˚LR growth of R- (in orange) in split-root plants (Figure 11). A
796 global transcriptome analysis identified local and systemic regulation of genes
797 by Pi starvation. Hormones (ABA and JA) and sugars were involved in the
798 systemic response of RSA to Pi starvation, and ROS were involved in
799 protecting roots from Pi-starvation (Figure 11). These results provide new
800 insights to long-term Pi starvation responses by offering new evidence of ABA

and JA signalling pathway being involved in the systemic regulation of Pi starvation-induced changes in root system architecture and the mechanistic basis of plant adaptation to low and heterogeneous Pi availability.

Acknowledgements

This work was supported by the National Nature Science Foundation of China (Grants No. 31972498 and 32172662). We also acknowledge the National Key R&D Program of China (Grant No. 2017YFD0200200) and Applied Basic Research Fronts Program of Wuhan city (Grant No. 2018020401011302). PJW was supported by the Rural and Environment Science and Analytical Services Division (RESAS) of the Scottish Government.

Author contributions

Y.L. and L.S. designed research; Y.L., X.Y., H.L., W.W., C.W., G.D., F.X., S.W., H.C. performed research; Y.L., P.W. and J.H. analyzed data; Y.L., L.S., M.Y, S. S., J.H. and P.W. wrote the paper.

Conflicts of interest

The authors declare no conflicts of interest.

Data Availability

All data supporting the findings of this study are available within the paper and within its supplementary materials published online.

Supplementary data

Supplementary data are available at *JXB* online.

Table S1. Quality of sequencing data

Table S2. Primer sequences used in the RT-qPCR experiment

829 **Table S3** Functions and differential expression of genes regulated systemically
830 by Pi-starvation in *Brassica napus*
831 **Table S4.** Differentially expressed genes (DEGs) enriching GO terms of
832 ABA-activated and JA-mediated signalling pathways shown in Figure 5a
833 **Figure S1.** Expression of selected differentially expressed genes (DEGs) in
834 the roots of *B. napus* seedlings 9 DAT to the split-root systems illustrated in
835 Figure 1.
836 **Figure S2.** Expression of ten differentially expressed genes (DEGs) related to
837 hormone (JA and ABA) metabolism, sugar metabolism and oxidative stress in
838 the roots of *B. napus* seedlings 2 DAT to the split-root systems.
839 **Figure S3.** Cell activity of roots grown in the split-root systems illustrated in
840 Figure 1.

References

Anwar A, Bai L, Miao L, Liu Y, Li S, Yu X, Li Y. 2018. 24-epibrassinolide ameliorates endogenous hormone levels to enhance low-temperature stress tolerance in cucumber seedlings. International Journal of Molecular Sciences **19**, 2497.

Battal P, Turker M, Tileklio□lu B. 2003. Effects of different mineral nutrients on abscisic acid in maize (*Zea mays*). Annales Botanici Fennici **40**, 301–308.

Benitez-Alfonso Y, Jackson D, Maule A. 2011. Redox regulation of intercellular transport. Protoplasma **248**, 131–140.

Bouain N, Doumas P, Rouached H. 2016. Recent advances in understanding the molecular mechanisms regulating the root system response to phosphate deficiency in *Arabidopsis*. Current Genomics **17**, 308–314.

Bustos R, Castrillo G, Linhares F, Puga MI, Rubio V, Pérez-Pérez J, Solano R, Leyva A, Paz-Ares J. 2010. A central regulatory system largely controls transcriptional activation and repression responses to phosphate starvation in *Arabidopsis*. Plos Genetics **6**, e1001102.

Chacón-López A, Ibarra-Laclette E, Sánchez-Calderón L, Gutiérrez-Alanís D, Herrera-Estrella L. 2011. Global expression pattern comparison between *low phosphorus insensitive 4* and WT *Arabidopsis* reveals an important role of reactive oxygen species and jasmonic acid in the root tip response to phosphate starvation. Plant Signaling and Behavior **6**, 382–392.

Chen S, Ding G, Wang Z, Cai H, Xu F. 2015. Proteomic and comparative genomic analysis reveals adaptability of *Brassica napus* to phosphorus-deficient stress. Journal of Proteomics **117**, 106–119.

Chen S, Hajirezaei M, Peisker M, Tschiersch H, Sonnewald U, Börnke F. 2005. Decreased sucrose-6-phosphate phosphatase level in transgenic tobacco inhibits photosynthesis, alters carbohydrate partitioning, and reduces growth. Planta **221**, 479–492.

Chen ZY, Wang YT, Pan XB, Xi ZM. 2019. Amelioration of cold-induced oxidative stress by exogenous 24-epibrassinolide treatment in grapevine seedlings: Toward regulating the ascorbate–glutathione cycle. Scientia Horticulturae **244**, 379–387.

Chien PS, Chiang CP, Leong SJ, Chiou TJ. 2018. Sensing and signaling of

phosphate starvation: from local to long distance. Plant and Cell Physiology **59**, 1714–1722.

Chiou TJ, Lin SI. 2011. Signaling network in sensing phosphate availability in plants. Annual Review of Plant Biology **62**, 185–206.

Choudhury S, Panda P, Sahoo L, Panda SK. 2013. Reactive oxygen species signaling in plants under abiotic stress. Plant Signaling and Behavior **8**, e23681.

Choudhury FK, Rivero RM, Blumwald E, Mittler R. 2016. Reactive oxygen species, abiotic stress and stress combination. Plant Journal **90**, 856–867.

Ciereszko I, Johansson H, Kleczkowski LA. 2005. Interactive effects of phosphate deficiency, sucrose and light/dark conditions on gene expression of UDP-glucose pyrophosphorylase in *Arabidopsis*. Journal of Plant Physiology **162**, 343–353.

Dasgupta K, Khadilkar AS, Sulpice R, Pant B, Scheible WR, Fisahn J, Stitt M, Ayre BG. 2014. Expression of sucrose transporter cDNAs specifically in companion cells enhances phloem loading and long-distance transport of sucrose but leads to an inhibition of growth and the perception of a phosphate limitation. Plant Physiology **165**, 715–731.

Dunand C, Crèvecoeur M, Penel C. 2006. Distribution of superoxide and hydrogen peroxide in *Arabidopsis* root and their influence on root development: possible interaction with peroxidases. New Phytologist **174**, 332–341.

Fernández RC, Maresma BG, Juárez A, Martínez J. 2004. Production of fructooligosaccharides by *β*-fructofuranosidase from *Aspergillus* sp 27H. Journal of Chemical Technology and Biotechnology **79**, 268–272.

Feussner I, Wasternack C. 2002. The lipoxygenase pathway. Annual Review of Plant Biology **53**, 275–297.

Fonseca S, Chini A, Hamberg M, Adie B, Porzel A, Kramell R, Miersch O, Wasternack C, Solano R. 2009. (+)-7-iso-Jasmonoyl-L-isoleucine is the endogenous bioactive jasmonate. Nature Chemical Biology **5**, 344–350.

Franco-Zorrilla M, Martı AC, Leyva A, Paz-Ares J. 2005. Interaction between phosphate-starvation, sugar, and cytokinin signaling in *Arabidopsis* and the roles of cytokinin receptors CRE1/AHK4 and AHK3. Plant Physiology **138**, 847–857.

Funakoshi Y, Daimon H, Matsumura A. 2015. Formation of densely

branched lateral roots in *Sesbania cannabina* triggered by patchily distributed phosphorus in andosolic soils. Plant Root **9**, 24–33.

Gong Z, Xiong L, Shi H, Yang S, Zhu JK. 2020. Plant abiotic stress response and nutrient use efficiency. Science China Life Sciences **63**, 635–674.

Gutiérrez-Alanís D, Ojeda-Rivera JO, Yong-Villalobos L, Cárdenas-Torres L, Herrera-Estrella L. 2018. Adaptation to phosphate scarcity: tips from *Arabidopsis* roots. Trends in Plant Science **23**, 721–730.

Ha S, Tran LS. 2014. Understanding plant responses to phosphorus starvation for improvement of plant tolerance to phosphorus deficiency by biotechnological approaches. Critical Reviews in Biotechnology **34**, 16–30.

Haigler CH, Singh B, Zhang D, *et al.* 2007. Transgenic cotton over-producing spinach sucrose phosphate synthase showed enhanced leaf sucrose synthesis and improved fiber quality under controlled environmental conditions. Plant Molecular Biology **63**, 815–832.

Ham BK, Chen J, Yan Y, Lucas WJ. 2018. Insights into plant phosphate sensing and signaling. Current Opinion in Biotechnology **49**, 1–9.

Hammond JP, White PJ. 2008. Sucrose transport in the phloem: Integrating root responses to phosphorus starvation. Journal of Experimental Botany **59**, 93–109.

Hammond JP, White PJ. 2011. Sugar signaling in root responses to low phosphorus availability. Plant Physiology **156**, 1033–1040.

Hao Q, Yin P, Li W, Wang L, Yan C, Lin Z, Wu JZ, Wang J, Yan SF, Yan N. 2011. The molecular basis of ABA-independent inhibition of PP2Cs by a subclass of PYL proteins. Molecular Cell **42**, 662–672.

Hawkesford M, Horst W, Kichey T, Lambers H, Schjoerring J, Møller IS, White P. 2012. Marschner's Mineral Nutrition of Higher Plants. || Functions of Macronutrients. 135-189.

He J, Duan Y, Hua D, Fan G, Wang L, Liu Y, Chen Z, Han L, Qu LJ, Gonga Z. 2012. DEXH box RNA helicase-mediated mitochondrial reactive oxygen species production in *Arabidopsis* mediates crosstalk between abscisic acid and auxin signaling. Plant Cell **24**, 1815–1833.

Hermans C, Hammond JP, White PJ, Verbruggen N. 2006. How do plants respond to nutrient shortage by biomass allocation? Trends in Plant Science **11**, 610–617.

Jain A, Poling MD, Karthikeyan AS, Blakeslee JJ, Peer WA, Titapiwatanakun B, Murphy AS, Raghothama KG. 2007. Differential effects of sucrose and auxin on localized phosphate deficiency-induced modulation of different traits of root system architecture in *Arabidopsis*. Plant Physiology **144**, 232–247.

Jin K, White PJ, Whalley WR, Shen J, Shi L. 2017. Shaping an optimal soil by root–soil interaction. Trends in Plant Science **22**, 823–829.

Khan GA, Vogiatzaki E, Glauser G, Poirier Y. 2016. Phosphate deficiency induces the jasmonate pathway and enhances resistance to insect herbivory. Plant Physiology **171**, 632–644.

Lei M, Liu Y, Zhang B, Zhao Y, Wang X, Zhou Y, Raghothama KG, Liu D. 2011. Genetic and genomic evidence that sucrose is a global regulator of plant responses to phosphate starvation in *Arabidopsis*. Plant Physiology **156**, 1116–1130.

Li H, Ma Q, Li H, Zhang F, Rengel Z, Shen J. 2014. Root morphological responses to localized nutrient supply differ among crop species with contrasting root traits. Plant and Soil **376**, 151–163.

Lin WY, Huang TK, Leong SJ, Chiou TJ. 2014. Long-distance call from phosphate: systemic regulation of phosphate starvation responses. Journal of Experimental Botany **65**, 1817–1827.

Linkohr BI, Williamson LC, Fitter AH, Leyser HMO. 2002. Nitrate and phosphate availability and distribution have different effects on root system architecture of *Arabidopsis*. The Plant Journal **29**, 751–760.

Liu H, Li X, Xiao J, Wang S. 2012. A convenient method for simultaneous quantification of multiple phytohormones and metabolites: application in study of rice-bacterium interaction. Plant Methods **8**, 2.

Liu J, Samac DA, Bucciarelli B, Allan DL, Vance CP. 2005. Signaling of phosphorus deficiency-induced gene expression in white lupin requires sugar and phloem transport. Plant Journal **41**, 257–268.

López-Bucio J, Hernández-Abreu E, Sánchez-Calderón L, Nieto-Jacobo MF, Simpson J, Herrera-Estrella L. 2002. Phosphate availability alters architecture and causes changes in hormone sensitivity in the Arabidopsis root system. Plant Physiology **129**, 244-256.

López-Bucio JS, Salmerón-Barrera GJ, Ravelo-Ortega G, Raya-González

J, León P, de la Cruz HR, Campos-García J, López‐Bucio J, Guevara-García ÁA. 2019. Mitogen-activated protein kinase 6 integrates phosphate and iron responses for indeterminate root growth in *Arabidopsis thaliana*. Planta **250**, 1177-1189.

Lynch JP. 2011. Root phenes for enhanced soil exploration and phosphorus acquisition: tools for future crops. Plant Physiology **156**, 1041–1049.

Lynch JP, Wojciechowski T. 2015. Opportunities and challenges in the subsoil: pathways to deeper rooted crops. Journal of Experimental Botany **66**, 2199–2210.

Ma Y, Szostkiewicz I, Korte A, Moes D, Yang Y, Christmann A, Grill E. 2009. Regulators of PP2C phosphatase activity function as abscisic acid sensors. Science **324**, 1064–1068.

Mosblech A, Thurow C, Gatz C, Feussner I, Heilmann I. 2011. Jasmonic acid perception by COI1 involves inositol polyphosphates in *Arabidopsis thaliana*. Plant Journal **65**, 949–957.

Müller R, Morant M, Jarmer H, Nilsson L, Nielsen TH. 2007. Genome-wide analysis of the *Arabidopsis* leaf transcriptome reveals interaction of phosphate and sugar metabolism. Plant Physiology **143**, 156–171.

Müller J, Toev T, Heisters M, Teller J, Moore KL, Hause G, Dinesh DC, Bürstenbinder K, Abel S. 2015. Iron-dependent callose deposition adjusts root meristem maintenance to phosphate availability. Developmental Cell **33**, 216–230.

Obersteiner M, Peñuelas J, Ciais P, Van Der Velde M, Janssens IA. 2013. The phosphorus trilemma. Nature Geoscience **6**, 897–898.

Oldroyd GED, Leyser O. 2020. A plant's diet, surviving in a variable nutrient environment. Science **368**, eaba0196.

Pant BD, Pant P, Erban A, Huhman D, Kopka J, Scheible WR. 2015. Identification of primary and secondary metabolites with phosphorus status-dependent abundance in *Arabidopsis*, and of the transcription factor PHR1 as a major regulator of metabolic changes during phosphorus limitation. Plant Cell and Environment **38**, 172–187.

Péret B, Desnos T, Jost R, Kanno S, Berkowitz O, Nussaume L. 2014. Root architecture responses: in search of phosphate. Plant Physiology **166**, 1713–1723.

Pérez-Torres CA, López-Bucio J, Cruz-Ramírez A, Ibarra-Laclette E, Dharmasiri S, Estelle M, Herrera-Estrella L. 2008. Phosphate availability alters lateral root development in *Arabidopsis* by modulating auxin sensitivity via a mechanism involving the TIR1 Auxin Receptor. Plant Cell **20**, 3258-3272.

Péret B, De Rybel B, Casimiro I, Benková E, Swarup R, Laplaze L, Beeckman T, Bennett MJ. 2009. *Arabidopsis* lateral root development: an emerging story. Trends in Plant Science **14**, 399-408.

Puga MI, Rojas-Triana M, de Lorenzo L, Leyva A, Rubio V, Paz-Ares J. 2017. Novel signals in the regulation of Pi starvation responses in plants: facts and promises. Current Opinion in Plant Biology **39**, 40–49.

Ravelo-Ortega G, Pelagio-Flores R, López-Bucio J, Campos-García J, de la Cruz RH, López-Bucio JS. 2022. Early sensing of phosphate deprivation triggers the formation of extra root cap cell layers via SOMBRERO through a process antagonized by auxin signaling. Plant Molecular Biology **108**,77-91.

Raya-González J, Ojeda-Rivera JO, Mora-Macias J, Oropeza-Aburto A, Ruiz-Herrera LF, López-Bucio J, Herrera-Estrella L. 2021. MEDIATOR16 orchestrates local and systemic responses to phosphate scarcity in *Arabidopsis* roots. New Phytologist **229**, 1278-1288.

Richardson AE, Simpson RJ. 2011. Soil microorganisms mediating phosphorus availability**.** Plant physiology **156**, 989–996.

Rubio V, Bustos R, Irigoyen ML, Cardona-López X, Rojas-Triana M, Paz-Ares J. 2009. Plant hormones and nutrient signaling. Plant Molecular Biology **69**, 361–373.

Ruiz-Herrera LF, Shane MW , López-Bucio J. 2015. Nutritional regulation of root development. Wiley Interdisciplinary Reviews Developmental Biology **4**, 431–443.

Sánchez-Calderón L, López-Bucio J, Chacón-López A, Cruz-Ramírez A, Nieto-Jacobo F, Dubrovsky JG, Herrera-Estrella L. 2005. Phosphate starvation induces a determinate developmental program in the roots of *Arabidopsis thaliana*. Plant and Cell Physiology **46**, 174–184.

Santos TMM dos, Ślaski JJ, Carvalho MÂAP de, Lor G ory JT, Maria R. Clemente Vieira. 2005. Evaluating the Madeiran wheat germplasm for aluminum resistance using aluminium-induced callose formation in root apices as a marker. Acta Physiologiae Plantarum **27**, 297–302.

Schaller F. 2001. Enzymes of the biosynthesis of octadecanoid-derived signalling molecules. Journal of Experimental Botany **52**, 11–23.

Shan X, Zhang Y, Peng W, Wang Z, Xie D. 2009. Molecular mechanism for jasmonate-induction of anthocyanin accumulation in *Arabidopsis*. Journal of Experimental Botany **60**, 3849–3860.

Shen J, Li H, Neumann G, Zhang F. 2005. Nutrient uptake, cluster root formation and exudation of protons and citrate in *Lupinus albus* as affected by localized supply of phosphorus in a split-root system. Plant Science **168**, 837–845

Shi L, Shi TX, Broadley MR, White PJ, Long Y, Meng JL, Xu FS, Hammond JP. 2013. High-throughput root phenotyping screens identify genetic loci associated with root architectural traits in *Brassica napus* under contrasting phosphate availabilities. Annals of Botany **112**, 381-389.

Shin R, Berg RH, Schachtman DP. 2005. Reactive oxygen species and root hairs in *Arabidopsis* root response to nitrogen, phosphorus and potassium deficiency. Plant and Cell Physiology **46**, 1350–1357.

Sobkowiak L, Bielewicz D, Malecka EM, Jakobsen I, Albrechtsen M, Szweykowska-Kulinska Z, Pacak A. 2012. The role of the P1BS element containing promoter-driven genes in Pi transport and homeostasis in plants. Frontiers in Plant Science **3**, 58.

Song JM, Guan Z, Hu J, *et al.* 2020. Eight high-quality genomes reveal pan-genome architecture and ecotype differentiation of *Brassica napus*. Nature Plants **6**, 34–45.

Sun F, Fan G, Hu Q, *et al.* 2017. The high-quality genome of *Brassica napus* cultivar 'ZS11' reveals the introgression history in semi-winter morphotype. Plant Journal **92**, 452–468.

Sun B, Gao Y, Lynch JP. 2018. Large crown root number improves topsoil foraging and phosphorus acquisition. Plant Physiology **177**, 90–104.

Sun L, Sun Y, Zhang M, *et al.* 2012. Suppression of 9-*cis*-epoxycarotenoid dioxygenase, which encodes a key enzyme in abscisic acid biosynthesis, alters fruit texture in transgenic tomato. Plant Physiology **158**, 283–298.

Svistoonoff S, Creff A, Reymond M, Sigoillot-Claude C, Ricaud L, Blanchet A, Nussaume L, Desnos T. 2007. Root tip contact with low-phosphate media reprograms plant root architecture. Nature Genetics **39**,

792–796.

Takahashi F, Suzuki T, Osakabe Y, Betsuyaku S, Kondo Y, Dohmae N, Fukuda H, Yamaguchi-Shinozaki K, Shinozaki K. 2018. A small peptide modulates stomatal control via abscisic acid in long-distance signaling. Nature **556**, 235–238.

Thibaud MC, Arrighi JF, Bayle V, Chiarenza S, Creff A, Bustos R, Paz-Ares J, Poirier Y, Nussaume L. 2010. Dissection of local and systemic transcriptional responses to phosphate starvation in *Arabidopsis*. Plant Journal **64**, 775–789.

Ticconi CA, Lucero RD, Sakhonwasee S, Adamson AW, Creff A, Nussaume L, Desnos T, Abel S. 2009. ER-resident proteins PDR2 and LPR1 mediate the developmental response of root meristems to phosphate availability. Proceedings of the National Academy of Sciences **106**, 14174–14179.

Trachsel S, Kaeppler SM, Brown KM, Lynch JP. 2011. Shovelomics: high throughput phenotyping of maize (*Zea mays* L.) root architecture in the field. Plant and Soil **341**, 75–87.

Tyburski J, Dunajska K, Tretyn A. 2009. Reactive oxygen species localization in roots of *Arabidopsis thaliana* seedlings grown under phosphate deficiency. Plant Growth Regulation **59**, 27–36.

Vanacker H, Carver TLW, Foyer CH. 2000. Early H_2O_2 accumulation in mesophyll cells leads to induction of glutathione during the hyper-sensitive response in the barley-powdery mildew interaction. Plant Physiology **123**, 1289–1300.

van der Bom FJT, Williams A, Bell MJ. 2020. Root architecture for improved resource capture: trade-offs in complex environments. Journal of Experimental Botany **71**, 5752-5763

Wang X, Feng J, White PJ, Shen J, Cheng L. 2019. Heterogeneous phosphate supply influences maize lateral root proliferation by regulating auxin redistribution. Annals of Botany **125**, 119–130.

Wang C, Huang W, Ying Y, Li S, Secco D, Tyerman S, Whelan J, Shou H. 2012. Functional characterization of the rice *SPX-MFS* family reveals a key role of *OsSPX-MFS1* in controlling phosphate homeostasis in leaves. New Phytologist **196**, 139–148.

Wang W Bin, Kim YH, Lee HS, Kim KY, Deng XP, Kwak SS. 2009. Analysis of antioxidant enzyme activity during germination of alfalfa under salt and drought stresses. Plant Physiology and Biochemistry **47**, 570–577.

Wang J, Qin Q, Pan J, Sun L, Sun Y, Xue Y, Song K. 2019. Transcriptome analysis in roots and leaves of wheat seedlings in response to low-phosphorus stress. Scientific Reports **9**, 19802.

Wang Q, Wang J, Yang Y, Du W, Zhang D, Yu D, Cheng H. 2016. A genome-wide expression profile analysis reveals active genes and pathways coping with phosphate starvation in soybean. BMC Genomics **17**, 1–11.

Williamson LC, Ribrioux SPCP, Fitter AH, Ottoline Leyser HM. 2001. Phosphate availability regulates root system architecture in *Arabidopsis*. Plant Physiology **126**, 875–882.

Woo J, MacPherson CR, Liu J, Wang H, Kiba T, Hannah MA, Wang XJ, Bajic VB, Chua NH. 2012. The response and recovery of the *Arabidopsis thaliana* transcriptome to phosphate starvation. BMC Plant Biology **12**, 1–22.

Xue Y, Zhuang Q, Zhu S, Xiao B, Liang C, Liao H, Tian J. 2018. Genome wide transcriptome analysis reveals complex regulatory mechanisms underlying phosphate homeostasis in soybean nodules. International Journal of Molecular Sciences **19**, 2924.

Yamamoto Y, Kobayashi Y, Devi SR, Rikiishi S, Matsumoto H. 2002. Aluminum toxicity is associated with mitochondrial dysfunction and the production of reactive oxygen species in plant cells. Plant Physiology **128**, 63–72.

Yang DL, Yao J, Mei CS, *et al.* 2012. Plant hormone jasmonate prioritizes defense over growth by interfering with gibberellin signaling cascade. Proceedings of the National Academy of Sciences of the United States of America **109**, E1192–E1200.

Zhang T, Hong Y, Wen XP. 2020. Over-expression of masson pine *PmPT1* gene in transgenic tobacco confers tolerance enhancement to Pi deficiency by ameliorating P level and the antioxidants. Plant Molecular Biology Reporter **38**, 238–249.

Zhang M, Leng P, Zhang G, Li X. 2009. Cloning and functional analysis of 9-*cis*-epoxycarotenoid dioxygenase (NCED) genes encoding a key enzyme during abscisic acid biosynthesis from peach and grape fruits. Journal of Plant

Physiology **166**, 1241–1252.

Zhang Y, Zhou Z, Yang Q. 2013. Genetic variations in root morphology and phosphorus efficiency of *Pinus massoniana* under heterogeneous and homogeneous low phosphorus conditions. Plant and Soil **364**, 93–104.

Zhao L, Zhou T, Li X, Fan S, You L. 2013. Expression and characterization of GH3 β-Glucosidase from *Aspergillus niger* NL-1 with high specific activity, glucose inhibition and solvent tolerance. Microbiology **82**, 356–363.

Zhou L, Hou H, Yang T, Lian Y, Sun Y, Bian Z, Wang C. 2018. Exogenous hydrogen peroxide inhibits primary root gravitropism by regulating auxin distribution during *Arabidopsis* seed germination. Plant Physiology and Biochemistry **128**, 126–133.

Zhu JK. 2016. Abiotic stress signaling and responses in plants. Cell **167**, 313–324.

Figure 1. Growth, biomass, Pi concentration in shoot and root, and lateral root morphology of *B. napus* seedlings in the split-root experiments. (a) A schematic diagram of the experimental procedure of the split-root experiment. R++: roots exposed to homogenous P treatment (P+/P+); R--: homogenous treatment without P given to roots (P-/P-); R+: heterogenous P treatment, with a part of the roots system receiving adequate P supply (on the P+ side); R-: heterogenous P treatment, with a part of the roots system receiving no P. S++: Shoots grown on P+/P+ dishes; S+-: Shoots grown on P+/P- dishes; S--: Shoots grown on P-/P- dishes. (b) Shoot and root growth of seedlings 9 DAT (days after transplantation) to the split-root system. The white horizontal lines show the root tips when the seedlings were transplanted to the split-root system. The scale bar = 2 cm. (c) Fresh weights of shoots and roots. (d) Pi concentrations of shoots and roots. (e) 1˚LR (first-order lateral root) elongation rates, (f) 1˚LR lengths, (g) 2˚LR (second-order lateral root) numbers, (h) 2˚LR density (number of 2˚LR per 1˚LR cm), (i) 2˚LR average lengths, and (j) total 2˚LR lengths 9 DAT. Values are the means ± SE (n = 20 biological replicates, except for Pi concentration where n = 5 biological replicates, each replicate being a composite sample of 10 plants). In (e) asterisks indicate a significant difference in 1˚LR elongation rate between R++ and R--, and between R-- and R- (*$P < 0.05$, **$P < 0.01$; Student's *t*-test). A one-way ANOVA was carried out for the other data, and post hoc comparisons were conducted using the SPSS Tukey HSD test at $P < 0.05$ level. Significant differences are indicated by different letters above the bars.

867 **Figure 2.** Transcriptional analysis of roots of *B. napus* grown in the split-root
868 system shown in Figure 1. (a) Number of up-regulated and down-regulated
869 differentially expressed genes (DEGs) in the pairwise comparisons of R++ vs.
870 R--, R+ vs. R++, R- vs. R-- and R+ vs. R-. (b-g) Venn diagrams showing the
871 number of genes that were locally-induced (b) locally-repressed (c)
872 systemically-induced (d, e) and systemically-repressed (f, g) by Pi starvation.
873 The number of locally or systemically regulated genes is highlighted in red.
874 The height of columns on the schematic histograms in b-g show relative
875 expression levels of genes involved in the local or systemic regulation in roots.
876 (h) The proportion of the genes whose promoter contains PHR1 binding site
877 (P1BS, GNATATNC) in different groups of genes.

878 **Figure 3.** Distribution and function of the genes regulated locally (a) or
879 systemically (b) by Pi starvation in roots of *B. napus* detailed in Tables 1 and 2.
880 The number of genes in the corresponding function is shown. Grey and black
881 arrows outside the circle and semicircle at the center of the circle indicate
882 locally- or systemically- induced and repressed genes, respectively.

Figure 4. Differentially expressed genes (DEGs) induced systemically by Pi starvation in roots of *B. napus*. (a-b) Venn diagrams and heat map of systemically induced DEGs. (c) The top 20 GO terms in the category of biological process enriched in systemically-induced DEGs. (d) The top 10 KEGG pathways enriched in systemically induced DEGs. The X-axis indicates the enrichment factor. The dot color and size indicate the *q*-value and gene number as shown on the right, respectively.

Figure 5. ABA and JA-mediated signalling pathway components in roots of *B. napus* implicated in the response to Pi starvation. (a) A heatmap showing expression levels, based on relative FPKM values, of 18 genes in the GO terms of both the ABA-activated and JA-mediated signalling pathways (the top frame), 23 genes in the GO terms of the ABA-activated signalling pathway (the middle frame) and 25 genes in the GO terms of the JA-mediated signalling pathway (the bottom frame). The ID of *B. napus* genes are shown on the right. The color gradient scale on the right represents the normalized FPKM values. (b, c) ABA, (d, e) JA and (f, g) JA-Ile concentrations in shoots and roots 9 DAT to the split-root system. Values are the means ± SE (n = 6 biological replicates, each replicate being a composite sample of 10 plants). A one-way ANOVA was carried out for the whole data set, and post hoc comparisons were conducted using the SPSS Tukey HSD test at $P < 0.05$ level. Significant differences are indicated by different letters above the bars.

Figure 6. Effects of JA (1 µM) and DIECA (10 µM; diethyldithiocarbamic acid, a JA biosynthesis inhibitor) applied to the -P compartment on the biomass and lateral root morphology of *B. napus* seedlings grown in a split-root system with heterogeneous Pi availability. (a) Shoot and root growth of the seedlings 9 DAT to the treatments. The white horizontal lines show the root tips position when the seedlings were transplanted to the split-root system. Scale bar = 2 cm. (b-c) Fresh weights of shoots and roots. (d) 1˚LR lengths, (e) 2˚LR numbers, (f) 2˚LR density, (g) 2˚LR average lengths, and (h) total 2˚LR lengths 9 DAT to the treatments. Values are the means ± SE (n = 20 biological replicates). A one-way ANOVA was carried out for the whole data set, and post hoc comparisons were conducted using the SPSS Tukey HSD test at $P < 0.05$ level. Significant differences are indicated by different letters above the bars.

Figure 7. Effects of ABA (5 µM) and FLD (3 µM; fluridone, an ABA biosynthesis inhibitor) applied to the -P compartment on the biomass and lateral root morphology of *B. napus* seedlings grown in a split-root system with heterogeneous Pi availability. (a) Shoot and root growth of the seedlings 9 DAT to the treatments. The white horizontal lines show the root tips position when the seedlings were transplanted to the split-root system. Scale bar = 2 cm. (b-c) Fresh weights of shoots and roots. (d) 1˚LR lengths, (e) 2˚LR numbers, (f) 2˚LR density, (g) 2˚LR average lengths, and (h) total 2˚LR lengths 9 DAT to the treatments. Values are the means ± SE (n = 20 biological replicates). A one-way ANOVA was carried out for the whole data set, and post hoc comparisons were conducted using the SPSS Tukey HSD test at $P < 0.05$ level. Significant differences are indicated by different letters above the bars.

Figure 8. The response of sugar metabolism in roots of *B. napus* to Pi starvation. (a) A heatmap showing the expression of differentially expressed genes (DEGs) induced systemically by Pi starvation in the KEGG pathway of starch and sucrose metabolism. The gene ID and gene function in *B. napus* are shown on the left and right, respectively. The gradient color barcode in the top right corner represents the normalized FPKM values. Concentrations of total soluble sugars (e,g, glucose, fructose, sucrose; b-c) and, specifically, sucrose (as an important systemic signal of plant P status; d-e) in shoots and roots 9 DAT to the split-root system. Values are the means ± SE (n = 5 biological replicates, each replicate being a composite sample of 10 plants). A one-way ANOVA was carried out for the whole data set, and post hoc comparisons were conducted using the SPSS Tukey HSD test at $P < 0.05$ level. Significant differences are indicated by different letters above the bars.

Figure 9. Effects of sucrose (1%) applied to the -P compartment on the biomass and lateral root morphology of *B. napus* seedlings grown in a split-root system with heterogeneous P availability. (a) Shoot and root growth of the seedlings 9 DAT to the split-root system. The white horizontal lines show the root tips position when the seedlings were transplanted to the split-root system. Scale bar = 2 cm. (b-c) Fresh weights of shoots and roots. (d) 1˚LR lengths, (e) 2˚LR numbers, (f) 2˚LR density, (g) 2˚LR average lengths, and (h) total 2˚LR lengths 9 DAT to the split-root system. Values are the means ± SE (n = 20 biological replicates). A one-way ANOVA was carried out for the whole data set, and post hoc comparisons were conducted using the SPSS Tukey HSD test at $P < 0.05$ level. Significant differences are indicated by different letters above the bars.

Figure 10. Modulation of the antioxidant system in roots of *B. napus* in response to Pi starvation. (a) A heatmap showing the expression of 28 differentially expressed genes (DEG), based on relative FPKM values, in the GO term of response to oxidative stress. The gene ID and gene function in *B. napus* are shown on the left and right, respectively. The gradient colour barcode in the top right corner represents normalized FPKM values. (b) In situ accumulation of H_2O_2 (the upper row), O_2^- (the middle row) and callose (the bottom row) in the root tips as revealed by histochemical staining with DAB, DHE and aniline blue, respectively. Scale bar = 200 μm. (c) Quantification of DAB reactive staining intensity, relative fluorescent intensity of DHE and aniline blue in the root, respectively (n ≥ 20). (d, e) Activities of POD (d) and SOD (e) enzymes and (f) H_2O_2, (g) O_2^-, (h) callose and (i) MDA content in the root measured 9 DAT to the split-root system. Values are the means ± SE (n = 5 biological replicates, each replicate being a composite sample of 10 plants). A one-way ANOVA was carried out for the whole data set, and post hoc comparisons were conducted using the SPSS Tukey HSD test at $P < 0.05$ level. Significant differences are indicated by different letters above each column.

Figure 11. Schematic model for local and systemic signalling involved in the response of RSA of *B. napus* to homogeneous and heterogeneous Pi availability in a split-root system. We speculate that systemic signals for P supply and P demand regulate RSA when plants are exposed to heterogeneous Pi availability: systemic P-demand (−P) signalling promotes 2˚LR growth of R+ (in blue), systemic P-supply (+P) signalling inhibits 2˚LR growth of R- (in orange). Hormones (ABA and JA) and sugars are involved in the systemic response of RSA to Pi starvation. These systemic signals likely act in combination with local signals to regulate root development. "=" and "∓" indicate that the expression level of genes are either similar or significant different in roots of the two groups of plants.

982 **Table 1.** Function and differential expression of genes regulated locally by Pi-starvation in *Brassica napus* roots

Classification	FC			
	FC > 8	4 < FC < 8	2< FC < 4	
Locally-induced gene				
Hormone-related				
Gibberellin-regulated family protein			*BnA09g0343580.1*	
Ethylene-responsive element binding factor 15 (*ERF15*)			*BnC03g0556860.1*	
Ethylene response factor 1 (*ERF1*)			*BnA02g0074220.1*	*BnC03g0556860.1*
Ethylene response DNA binding factor 3 (*EDF3*)			*BnA02g0077520.1*	
Jasmonate-zim-domain protein 10 (*JAZ10*)		*BnA10g0414670.1*		
Ethylene-forming enzyme (*EFE*)			*BnC05g0688270.1*	
Zinc-finger protein 2 (*ZF2*)			*BnA03g0132100.1*	
Indole-3-acetic acid 7 (*IAA7*)			*BnC02g0502030.1*	
Indole-3-acetic acid inducible 29 (*IAA29*)			*BnA03g0154430.1*	
Auxin efflux carrier family protein (*PIN*)	*BnA07g0287850.1*			
Metal-related				
Matrixin family protein		*BnUnng1003600.1*	*BnA06g0236950.1*	
Heavy metal transport/detoxification superfamily protein		*BnC07g0792430.1*	*BnC01g0425370.1*	
Ferritin 3 (*FER3*)			*BnUnng0950990.1*	*BnA09g0373290.1*
			BnC08g0865140.1	
YELLOW STRIPE like 2 (*YSL2*)			*BnC07g0813840.1*	
Zinc transporter precursor (*ZIP*)		*BnUnng0946810.1*	*BnA01g0028880.1*	
Copper chaperone (*CCH*)			*BnA09g0373430.1*	
Farnesylated protein 3 (*FP3*)			*BnC09g0929170.1*	

Classification	FC			
	FC > 8	4 < FC < 8	2< FC < 4	
Stress-related				
Cytochrome P450	*BnC03g0530870.1*	*BnA08g0313800.1*	*BnC08g0863810.1*	*BnA08g0317030.1*
	BnC04g0672330.1	*BnA09g0386110.1*	*BnC03g0609930.1*	*BnC01g0450440.1*
Disease resistance protein family		*BnC03g0560400.1*	*BnC01g0452050.1*	*BnC02g0477310.1*
Response to stress protein			*BnC04g0626250.1*	*BnA03g0140120.1*
			BnA08g0314910.1	
Transcription factors				
WRKY family transcription factor	*BnC05g0711350.1*	*BnC02g0475750.1*	*BnC01g0441220.1*	*BnA08g0317280.1*
	BnC03g0540540.1	*BnA10g0414810.1*	*BnA04g0181090.1*	*BnA03g0147830.1*
			BnC03g0561760.1	*BnA06g0250710.1*
			BnC07g0789510.1	*BnC03g0542280.1*
			BnUnng0945570.1	*BnA02g0052450.1*
			BnA03g0095590.1	*BnC09g0928650.1*
NAC domain containing protein	*BnA05g0214880.1*	*BnC09g0889430.1*	*BnUnng1000260.1*	*BnC04g0658660.1*
	BnC03g0581630.1	*BnC05g0723420.1*	*BnA01g0035980.1*	*BnA02g0045140.1*
	BnA02g0056610.1		*BnA02g0088360.1*	*BnA10g0414720.1*
			BnC03g0538780.1	
NAC-like		*BnC06g0763770.1*	*BnA07g0294910.1*	
Myb domain protein	*BnC01g0427060.1*	*BnA05g0186360.1*	*BnC03g0569850.1*	*BnC08g0880160.1*
		BnA02g0083870.1	*BnA09g0382840.1*	*BnC04g0634540.1*
		BnC09g0889670.1	*BnC08g0854560.1*	*BnA08g0322200.1*
			BnA02g0058610.1	*BnC07g0814160.1*
			BnA07g0272050.1	*BnC07g0786310.1*

Classification	FC			
	FC > 8	4 < FC < 8	2< FC < 4	
Myb-like transcription factor family protein			*BnA03g0143670.1*	*BnC02g0491140.1*
Homeodomain-like superfamily protein	*BnC08g0880540.1*	*BnA07g0284190.1*	*BnC03g0534210.1*	*BnA02g0046790.1*
			BnC03g0536670.1	
Homeobox-leucine zipper protein 3 (*HAT3*)			*BnC08g0868870.1*	
C2H2-type zinc finger family protein	*BnA02g0058540.1*	*BnA02g0058550.1*	*BnC03g0547480.1*	*BnC04g0676810.1*
Basic helix-loop-helix (bHLH) DNA-binding superfamily protein			*BnA09g0337080.1*	*BnA04g0162960.1*
			BnC01g0464080.1	*BnA05g0188540.1*
Integrase-type DNA-binding superfamily protein	*BnC07g0815890.1*	*BnC06g0757280.1*	*BnUnng0963640.1*	*BnC05g0714210.1*
PLATZ transcription factor family protein			*BnA07g0300540.1*	*BnC09g0892170.1*
Dof-type zinc finger DNA-binding family protein	*BnA02g0089590.1*		*BnA02g0067780.1*	
WUSCHEL related homeobox		*BnA02g0087930.1*		
		BnUnng0960070.1		
Transporter or traffic facilitator				
Nodulin MtN21/EamA-like transporter family protein		*BnC04g0652060.1*	*BnC08g0865700.1*	*BnC06g0747440.1*
			BnC04g0678440.1	
Major facilitator superfamily protein (*MFS*)	*BnA03g0112530.1*		*BnUnng0946560.1*	*BnA02g0050060.1*
			BnA06g0228180.1	*BnC02g0472890.1*
			BnA08g0333700.1	*BnA06g0250430.1*
			BnA05g0211860.1	*BnC02g0475290.1*
			BnUnng0977560.1	
Phosphate transporter 3;1 (*PHT3;1*)			*BnC09g0927650.1*	
Phosphate transporter traffic facilitator1 (*PHF1*)			*BnC08g0861530.1*	*BnC04g0654240.1*
Amino acid permease 4 (*AAP4*)		*BnA06g0249500.1*	*BnC09g0929350.1*	*BnA08g0308700.1*
MATE efflux family protein			*BnA03g0094220.1*	*BnA09g0384810.1*

Classification	FC			
	FC > 8	4 < FC < 8	2< FC < 4	
Sugar transporter (*STP*)		*BnC08g0883620.1*	*BnA09g0387420.1*	
		BnA09g0358900.1		
Cation/H^+ exchanger (*CHX*)		*BnC08g0862990.1*	*BnA08g0321080.1*	
ARM repeat superfamily protein	*BnC07g0837090.1*			
Detoxifying efflux carrier 35 (*DTX35*)			*BnUnng0944580.1*	
Dicarboxylate carrier 3 (*DIC3*)	*BnC03g0538850.1*			
Nucleotide-sugar transporter family protein	*BnC06g0755290.1*			
Non-intrinsic ABC protein 12 (*NAP12*)			*BnC03g0546880.1*	
NOD26-like intrinsic protein 1;2 (*NIP1;2*)			*BnA01g0011110.1*	
Oligopeptide transporter 9 (*OPT9*)	*BnC09g0913620.1*			
SNARE-like superfamily protein	*BnA07g0303360.1*			
Locally-repressed gene				
Growth, development				
Expansin	*BnA05g0190670.1*		*BnC06g0766230.1*	*BnA02g0044620.1*
			BnA07g0294990.1	*BnA02g0060570.1*
			BnA04g0175660.1	*BnC02g0517740.1*
			BnC04g0669040.1	*BnC07g0827020.1*
			BnA03g0152010.1	
Cellulase 3 (*CEL3*)			*BnA07g0295860.1*	
Cellulose synthase like (*CSLA7*)			*BnC04g0643300.1*	
Leucine-rich receptor-like protein kinase family protein			*BnA09g0379090.1*	*BnC08g0872370.1*
Cysteine-rich RLK (RECEPTOR-like protein kinase) (*CRK*)			*BnC03g0572510.1*	*BnC04g0656580.1*
Leucine-rich repeat (LRR) family protein			*BnA05g0209450.1*	*BnC09g0928830.1*

Classification	FC			
	FC > 8	4 < FC < 8	2< FC < 4	
Leucine-rich repeat protein kinase family protein	*BnA05g0204990.1*		*BnC07g0783470.1*	
Lateral root primordium (LRP) protein-related			*BnC01g0452890.1*	*BnA01g0027570.1*
			BnA07g0281960.1	
Root hair defective 6-like 4 (*RSL4*)			*BnC05g0711090.1*	
Plant regulator RWP-RK family protein			*BnA03g0151900.1*	
Hormone-related				
Gibberellin-regulated family protein		*BnA02g0058510.1*		
Gibberellin-oxidase	*BnA02g0063550.1*		*BnC04g0621660.1*	
BURP domain-containing protein			*BnC09g0891360.1*	
SAUR-like auxin-responsive protein family			*BnC01g0428740.1*	
Phosphatase 2C5 (*PP2C5*)		*BnC08g0856910.1*		
Indoleacetic acid-induced protein 16 (*IAA16*)			*BnUnng1013730.1*	
Metal-related				
2-oxoglutarate (2OG) and Fe (II)-dependent Oxygenase superfamily protein	*BnC03g0580110.1*		*BnA02g0072340.1*	*BnA06g0252990.1*
Root FNR 1 (*RFNR1*)			*BnUnng0944290.1*	
Heavy metal transport/detoxification superfamily protein		*BnA03g0136570.1*		
Vacuolar iron transporter (*VIT*) family protein			*BnA02g0072100.1*	
FER-like regulator of iron uptake			*BnC04g0640590.1*	*BnA07g0282910.1*
Copper transporter 2 (*COPT2*)			*BnC01g0456180.1*	
Potassium channel 3 (*AKT3*)			*BnA03g0154620.1*	
Metal tolerance protein A2 (*MTPA2*)			*BnC02g0476650.1*	
Sodium/calcium exchanger family protein/calcium-binding EF hand family protein			*BnA06g0224840.1*	

Classification	FC			
	FC > 8	4 < FC < 8	2< FC < 4	
Pi recycle				
HAD superfamily, subfamily IIIB acid phosphatase			*BnA03g0111260.1*	*BnC03g0561880.1*
Purple acid phosphatase 15 (*PAP15*)			*BnA01g0012910.1*	
Transcription factors				
Myb domain protein			*BnC03g0580070.1*	*BnA09g0340680.1*
			BnC09g0928930.1	*BnC09g0893670.1*
Myb-like HTH transcriptional regulator family protein			*BnA10g0419160.1*	
Basic helix-loop-helix (bHLH) DNA-binding family protein	*BnC04g0621110.1*	*BnA02g0079260.1*	*BnC03g0568170.1*	
		BnA07g0290920.1		
		BnA09g0374140.1		
Homeobox protein			*BnA10g0413110.1*	
Homeodomain-like superfamily protein	*BnC09g0913780.1*			
Duplicated homeodomain-like superfamily protein			*BnA03g0110860.1*	
Integrase-type DNA-binding superfamily protein			*BnA06g0255510.1*	*BnC03g0544530.1*
			BnC09g0891290.1	
NAC domain containing protein	*BnC04g0619940.1*	*BnA02g0049060.1*	*BnA03g0139350.1*	
K-box region and MADS-box transcription factor family protein	*BnA03g0106510.1*		*BnC09g0925990.1*	
P-loop containing nucleoside triphosphate hydrolases superfamily protein			*BnC04g0657250.1*	*BnA04g0160160.1*
AGAMOUS-like			*BnA02g0069020.1*	*BnA03g0096130.1*
			BnA01g0032040.1	
WRKY family transcription factor			*BnUnng0955050.1*	
GATA type zinc finger transcription factor family protein			*BnA03g0112190.1*	

Classification	FC			
	FC > 8	4 < FC < 8	2< FC < 4	
TBP-associated factor 5 (*TAF5*)			*BnA02g0085290.1*	
HY5-homolog (*HYH*)			*BnUnng0959450.1*	
C2H2-type zinc finger family protein			*BnC08g0866970.1*	
Basic leucine-zipper 7 (*bzip7*)			*BnC01g0426160.1*	
RAD-like 6 (*RL6*)	*BnA07g0299340.1*			
Transporter				
Major facilitator superfamily protein	*BnA07g0289640.1*	*BnC03g0561070.1*	*BnA07g0282080.1*	*BnA07g0289620.1*
			BnUnng0966600.1	*BnC04g0620600.1*
			BnA10g0404070.1	*BnC09g0893830.1*
H^+-ATPase 1 (*HA1*)		*BnA03g0153330.1*	*BnC07g0829770.1*	
Cation/H^+ exchanger 20 (*CHX20*)			*BnA09g0341200.1*	
Na^+/H^+ exchanger 1 (*NHX1*)			*BnC01g0453250.1*	
ABC transporter family protein	*BnC09g0904070.1*		*BnA06g0260600.1*	
ABC2 homolog 13 (*ATH13*)			*BnA06g0250820.1*	
ABC-2 type transporter family protein			*BnA04g0165490.1*	
Non-intrinsic ABC protein 14 (*NAP14*)			*BnC09g0927590.1*	
MATE efflux family protein		*BnA09g0383220.1*	*BnUnng1012830.1*	*BnC07g0805390.1*
Plasma membrane intrinsic protein (*PIP*)	*BnC09g0920100.1*		*BnA01g0036970.1*	
Transmembrane amino acid transporter family protein			*BnC02g0475860.1*	*BnC08g0838640.1*
Amino acid permease (*AAP*)			*BnC04g0645270.1*	*BnUnng1012390.1*
Inositol transporter (*INT*)			*BnC04g0622990.1*	*BnA01g0022340.1*
Atpase E1-E2 type family protein/haloacid dehalogenase-like hydrolase family protein		*BnC06g0744860.1*		
Tonoplast intrinsic protein 2;2 (*TIP2;2*)			*BnA01g0021060.1*	

Classification	FC		
	FC > 8	4 < FC < 8	2< FC < 4
Proton gradient regulation 5 (*PGR5*)			*BnA03g0137840.1*
Ammonium transporter 1;3 (*AMT1;3*)			*BnA07g0272070.1*
Nitrate transporter 1.1 (*NRT1.1*)		*BnA06g0232010.1*	
CBL-interacting protein kinase 23 (*CIPK23*)			*BnC05g0711790.1*
Sulfate transporter 1;2 (*SMLTR1;2*)			*BnC02g0499990.1*
Photosynthetic electron transfer C (*PETC*)			*BnC03g0572990.1*
CBS domain-containing protein			*BnA03g0099600.1*
Nodulin MtN21 /EamA-like transporter family protein		*BnA09g0350870.1*	
NOD26-like intrinsic protein 3;1 (*NIP3;1*)			*BnA08g0312780.1*
Dicarboxylate transporter 1 (*DiT1*)			*BnA10g0414990.1*

Note: Genes are classified according to their level of induction or repression (FC > 8, 4 < FC < 8 or 2 < FC < 4; FC, fold change). For induced genes, FC = R--/R++; for repressed genes, FC = R++/R--

Figure 1

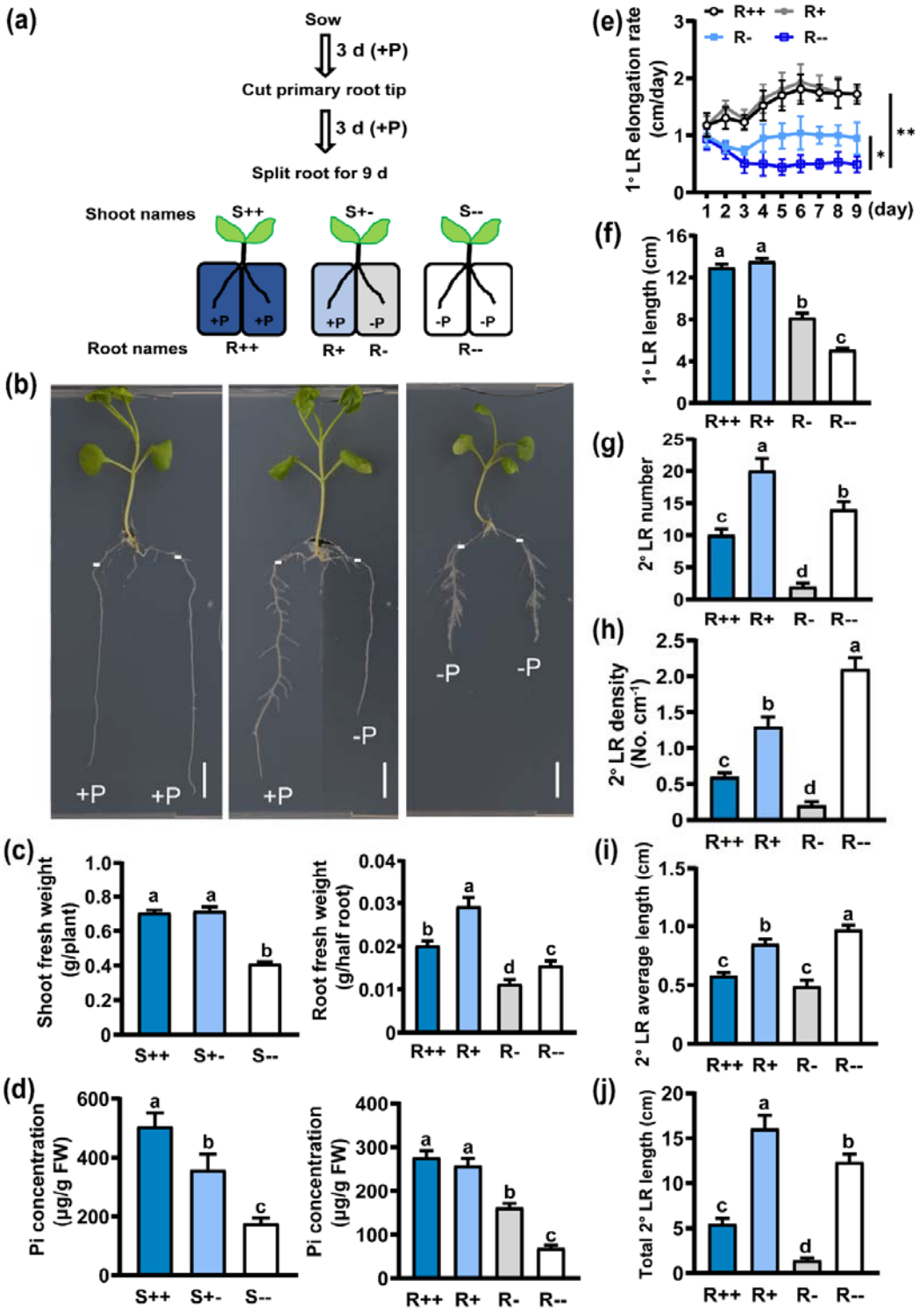

Figure 1. Growth, biomass, Pi concentration in shoot and root, and lateral root morphology of *B. napus* seedlings in the split-root experiments. (a) A

schematic diagram of the experimental procedure of the split-root experiment. R++: roots exposed to homogenous P treatment (P+/P+); R--: homogenous treatment without P given to roots (P-/P-); R+: heterogenous P treatment, with a part of the roots system receiving adequate P supply (on the P+ side); R-: heterogenous P treatment, with a part of the roots system receiving no P. S++: Shoots grown on P+/P+ dishes; S+-: Shoots grown on P+/P- dishes; S--: Shoots grown on P-/P- dishes. (b) Shoot and root growth of seedlings 9 DAT (days after transplantation) to the split-root system. The white horizontal lines show the root tips when the seedlings were transplanted to the split-root system. The scale bar = 2 cm. (c) Fresh weights of shoots and roots. (d) Pi concentrations of shoots and roots. (e) 1˚LR (first-order lateral root) elongation rates, (f) 1˚LR lengths, (g) 2˚LR (second-order lateral root) numbers, (h) 2˚LR density (number of 2˚LR per 1˚LR cm), (i) 2˚LR average lengths, and (j) total 2˚LR lengths 9 DAT. Values are the means ± SE (n = 20 biological replicates, except for Pi concentration where n = 5 biological replicates, each replicate being a composite sample of 10 plants). In (e) asterisks indicate a significant difference in 1˚LR elongation rate between R++ and R--, and between R-- and R- (*$P < 0.05$, **$P < 0.01$; Student's *t*-test). A one-way ANOVA was carried out for the other data, and post hoc comparisons were conducted using the SPSS Tukey HSD test at $P < 0.05$ level. Significant differences are indicated by different letters above the bars.

Figure 2

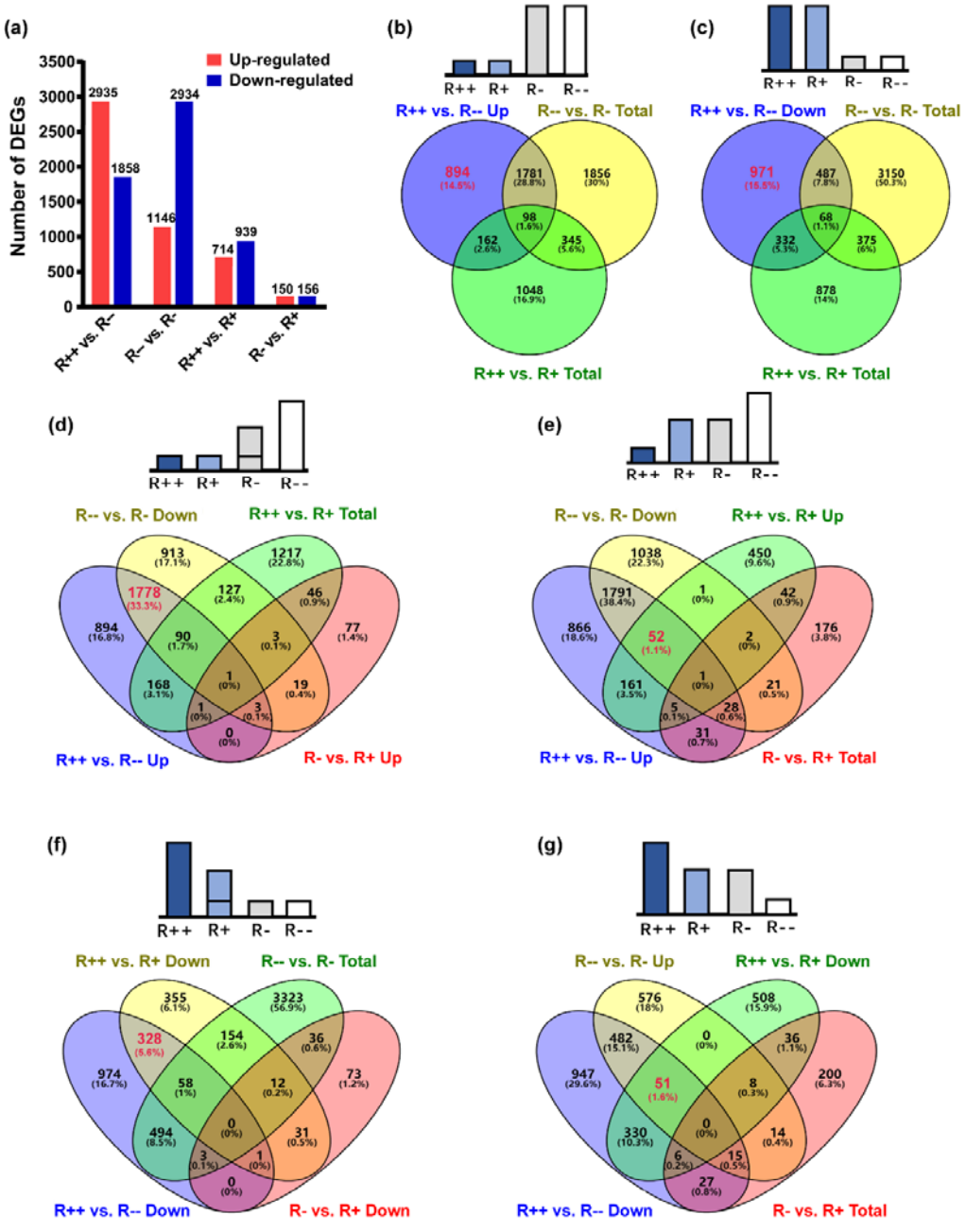

(h)

	Local induced genes	Local repressed genes	Systemic induced genes		Systemic repressed genes	
	(b)	(c)	(d)	(e)	(f)	(g)
Proportion of P1BS	37%	38%	83%	41%	36%	20%

Figure 2. Transcriptional analysis of roots of *B. napus* grown in the split-root system shown in Figure 1. (a) Number of up-regulated and down-regulated differentially expressed genes (DEGs) in the pairwise comparisons of R++ vs.

R--, R+ vs. R++, R- vs. R-- and R+ vs. R-. (b-g) Venn diagrams showing the number of genes that were locally-induced (b) locally-repressed (c) systemically-induced (d, e) and systemically-repressed (f, g) by Pi starvation. The number of locally or systemically regulated genes is highlighted in red. The height of columns on the schematic histograms in b-g show relative expression levels of genes involved in the local or systemic regulation in roots. (h) The proportion of the genes whose promoter contains PHR1 binding site (P1BS, GNATATNC) in different groups of genes.

Figure 3

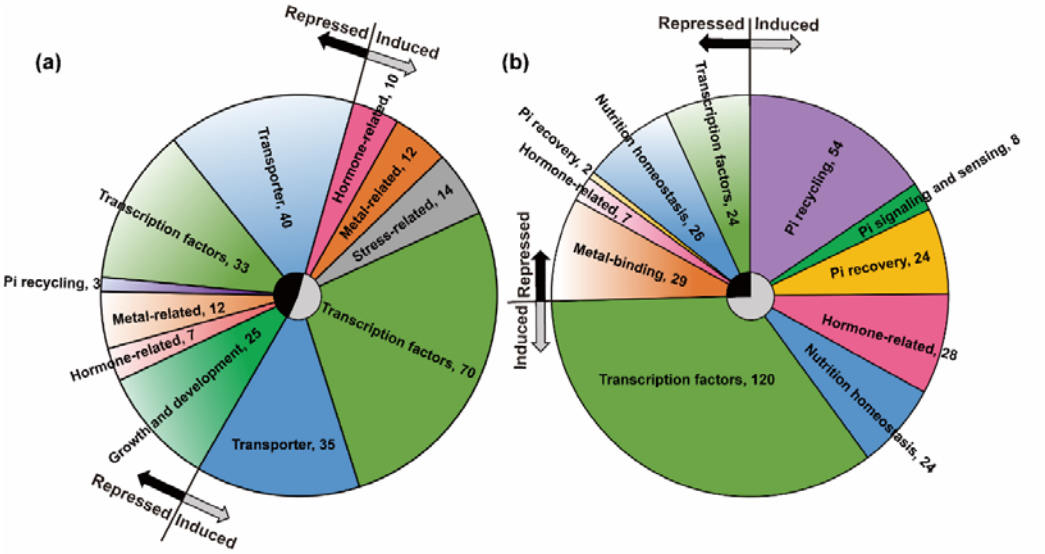

Figure 3. Distribution and function of the genes regulated locally (a) or systemically (b) by Pi starvation in roots of *B. napus* detailed in Tables 1 and 2. The number of genes in the corresponding function is shown. Grey and black arrows outside the circle and semicircle at the center of the circle indicate locally- or systemically- induced and repressed genes, respectively.

Figure 4

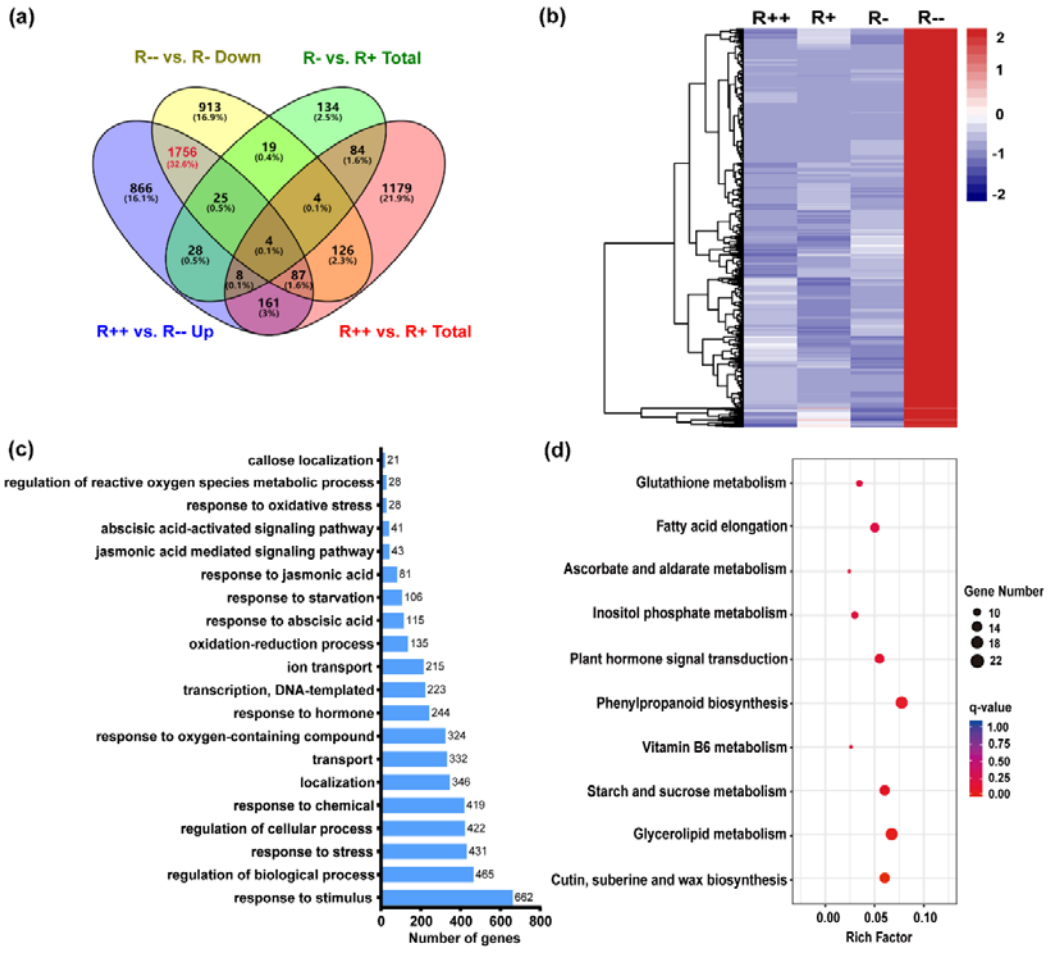

Figure 4. Differentially expressed genes (DEGs) induced systemically by Pi starvation in roots of *B. napus*. (a-b) Venn diagrams and heat map of systemically induced DEGs. (c) The top 20 GO terms in the category of biological process enriched in systemically-induced DEGs. (d) The top 10 KEGG pathways enriched in systemically induced DEGs. The X-axis indicates the enrichment factor. The dot color and size indicate the *q*-value and gene number as shown on the right, respectively.

Figure 5

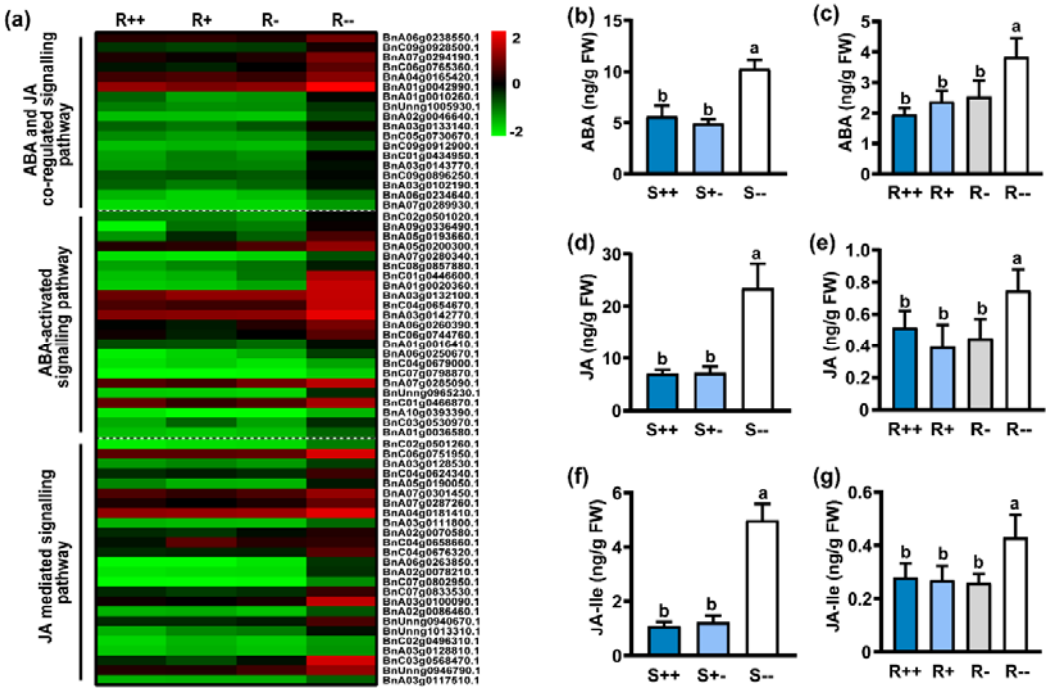

Figure 5. ABA and JA-mediated signalling pathway components in roots of *B. napus* implicated in the response to Pi starvation. (a) A heatmap showing expression levels, based on relative FPKM values, of 18 genes in the GO terms of both the ABA-activated and JA-mediated signalling pathways (the top frame), 23 genes in the GO terms of the ABA-activated signalling pathway (the middle frame) and 25 genes in the GO terms of the JA-mediated signalling pathway (the bottom frame). The ID of *B. napus* genes are shown on the right. The color gradient scale on the right represents the normalized FPKM values. (b, c) ABA, (d, e) JA and (f, g) JA-Ile concentrations in shoots and roots 9 DAT to the split-root system. Values are the means ± SE (n = 6 biological replicates, each replicate being a composite sample of 10 plants). A one-way ANOVA was carried out for the whole data set, and post hoc comparisons were conducted using the SPSS Tukey HSD test at $P < 0.05$ level. Significant differences were indicated by different letters above the bars.

Figure 6

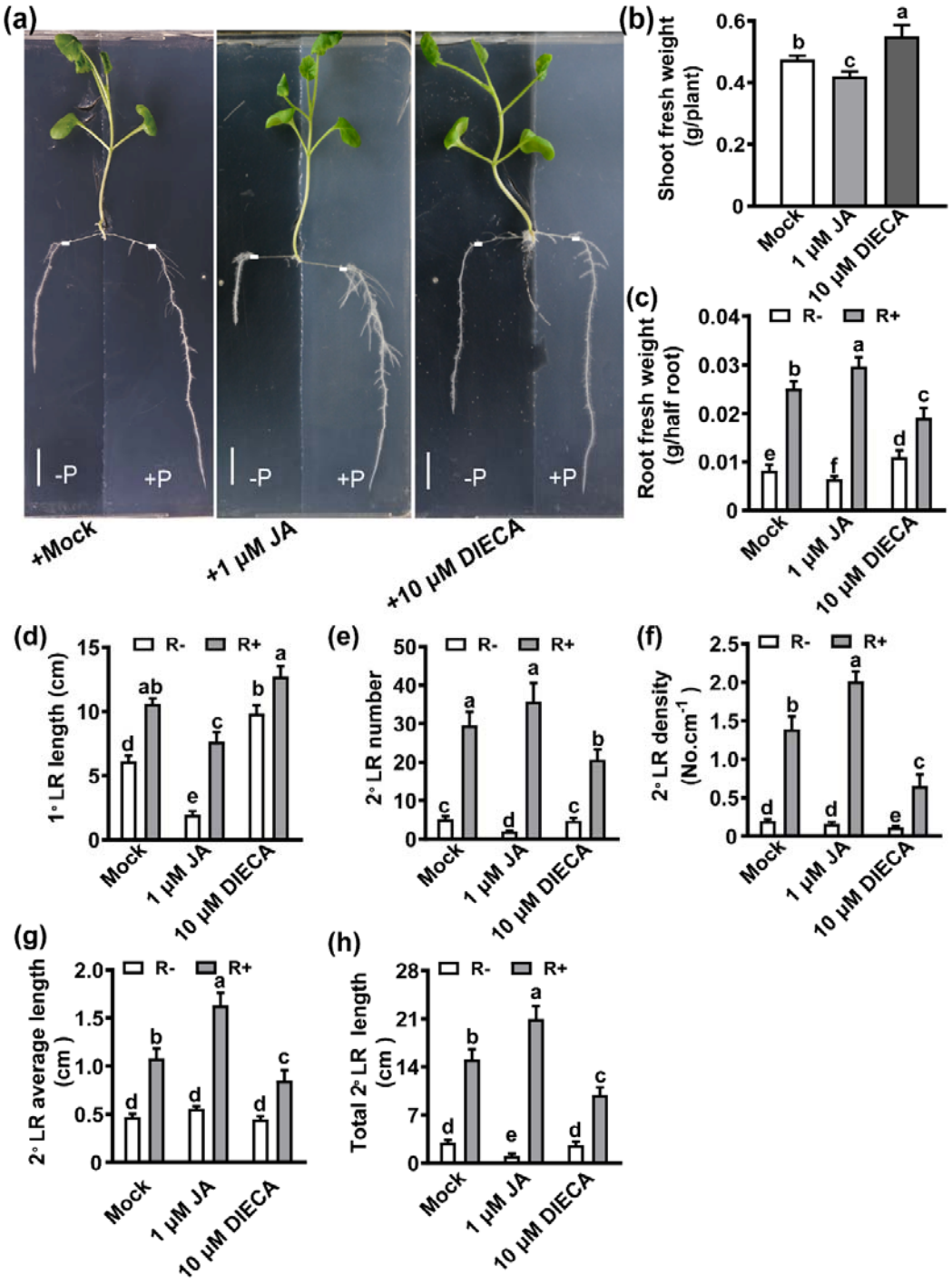

Figure 6. Effects of JA (1 μM) and DIECA (10 μM; diethyldithiocarbamic acid, a JA biosynthesis inhibitor) applied to the -P compartment on the biomass and lateral root morphology of *B. napus* seedlings grown in a split-root system with heterogeneous Pi availability. (a) Shoot and root growth of the seedlings 9 DAT to the treatments. The white horizontal lines show the root tips position when the seedlings were transplanted to the split-root system. Scale bar = 2 cm. (b-c)

Fresh weights of shoots and roots. (d) 1˚LR lengths, (e) 2˚LR numbers, (f) 2˚LR density, (g) 2˚LR average lengths, and (h) total 2˚LR lengths 9 DAT to the treatments. Values are the means ± SE (n = 20 biological replicates). A one-way ANOVA was carried out for the whole data set, and post hoc comparisons were conducted using the SPSS Tukey HSD test at $P < 0.05$ level. Significant differences are indicated by different letters above the bars.

Figure 7

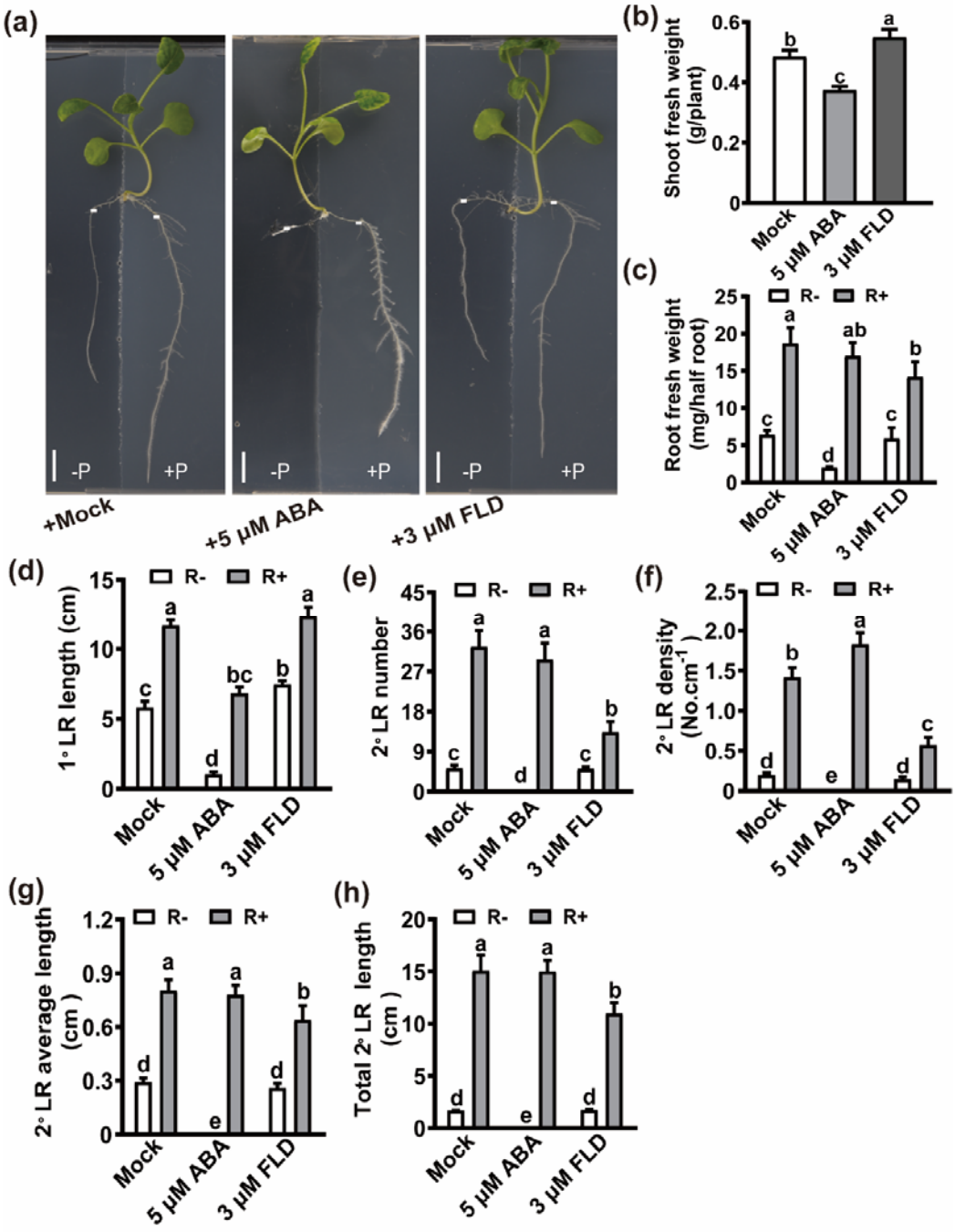

Figure 7. Effects of ABA (5 μM) and FLD (3 μM; fluridone, an ABA biosynthesis inhibitor) applied to the -P compartment on the biomass and lateral root morphology of *B. napus* seedlings grown in a split-root system with heterogeneous Pi availability. (a) Shoot and root growth of the seedlings 9 DAT to the treatments. The white horizontal lines show the root tips position when the seedlings were transplanted to the split-root system. Scale bar = 2 cm. (b-c)

Fresh weights of shoots and roots. (d) 1˚LR lengths, (e) 2˚LR numbers, (f) 2˚LR density, (g) 2˚LR average lengths, and (h) total 2˚LR lengths 9 DAT to the treatments. Values are the means ± SE (n = 20 biological replicates). A one-way ANOVA was carried out for the whole data set, and post hoc comparisons were conducted using the SPSS Tukey HSD test at $P < 0.05$ level. Significant differences are indicated by different letters above the bars.

Figure 8

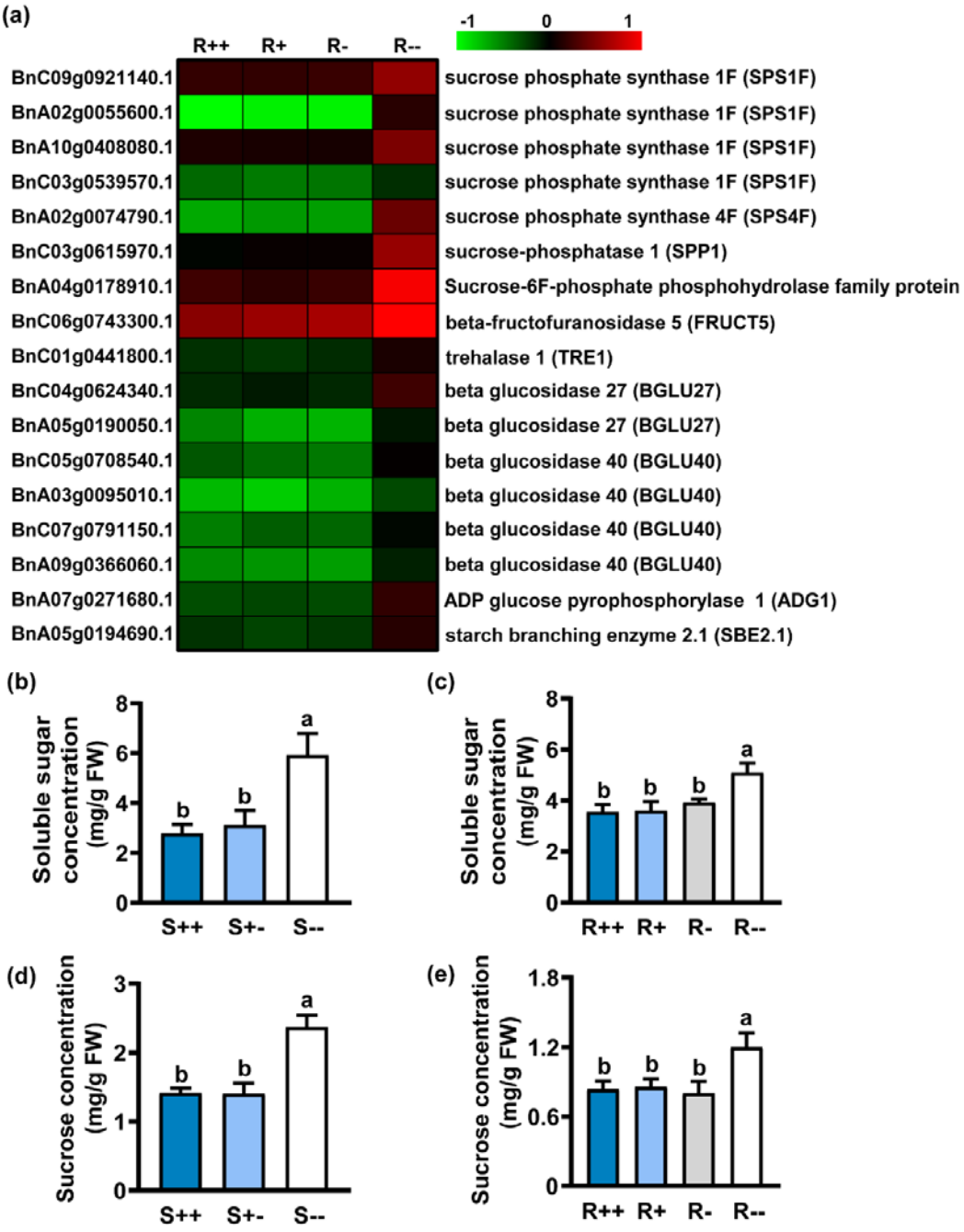

Figure 8. The response of sugar metabolism in roots of *B. napus* to Pi starvation. (a) A heatmap showing the expression of differentially expressed genes (DEGs) induced systemically by Pi starvation in the KEGG pathway of starch and sucrose metabolism. The gene ID and gene function in *B. napus* are shown on the left and right, respectively. The gradient color barcode in the top right corner represents the normalized FPKM values. Concentrations of total soluble sugars (e,g, glucose, fructose, sucrose; b-c) and, specifically,

sucrose (as an important Pi signalling; d-e) in shoots and roots 9 DAT to the split-root system. Values are the means ± SE (n = 5 biological replicates, each replicate being a composite sample of 10 plants). A one-way ANOVA was carried out for the whole data set, and post hoc comparisons were conducted using the SPSS Tukey HSD test at $P < 0.05$ level. Significant differences were indicated by different letters above the bars.

Figure 9

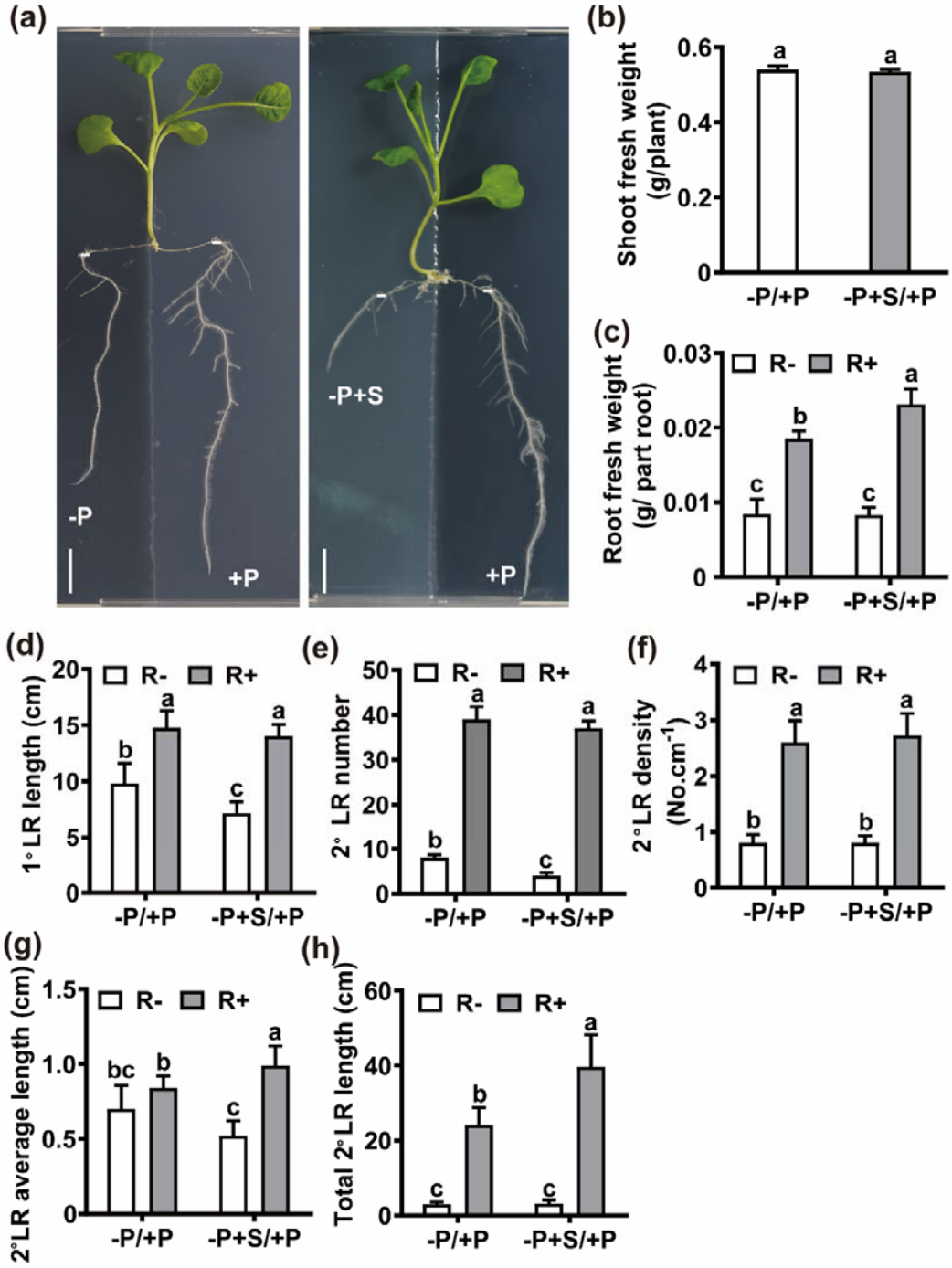

Figure 9. Effects of sucrose (1%) applied to the -P compartment on the biomass and lateral root morphology of *B. napus* seedlings grown in a split-root system with heterogeneous P availability. (a) Shoot and root growth of the seedlings 9 DAT to the split-root system. The white horizontal lines show the root tips position when the seedlings were transplanted to the split-root system. Scale bar = 2 cm. (b-c) Fresh weights of shoots and roots. (d) 1˚LR lengths, (e) 2˚LR numbers, (f) 2˚LR density, (g) 2˚LR average lengths, and (h)

total 2°LR lengths 9 DAT to the split-root system. Values are the means ± SE (n = 20 biological replicates). A one-way ANOVA was carried out for the whole data set, and post hoc comparisons were conducted using the SPSS Tukey HSD test at $P < 0.05$ level. Significant differences are indicated by different letters above the bars.

Figure 10

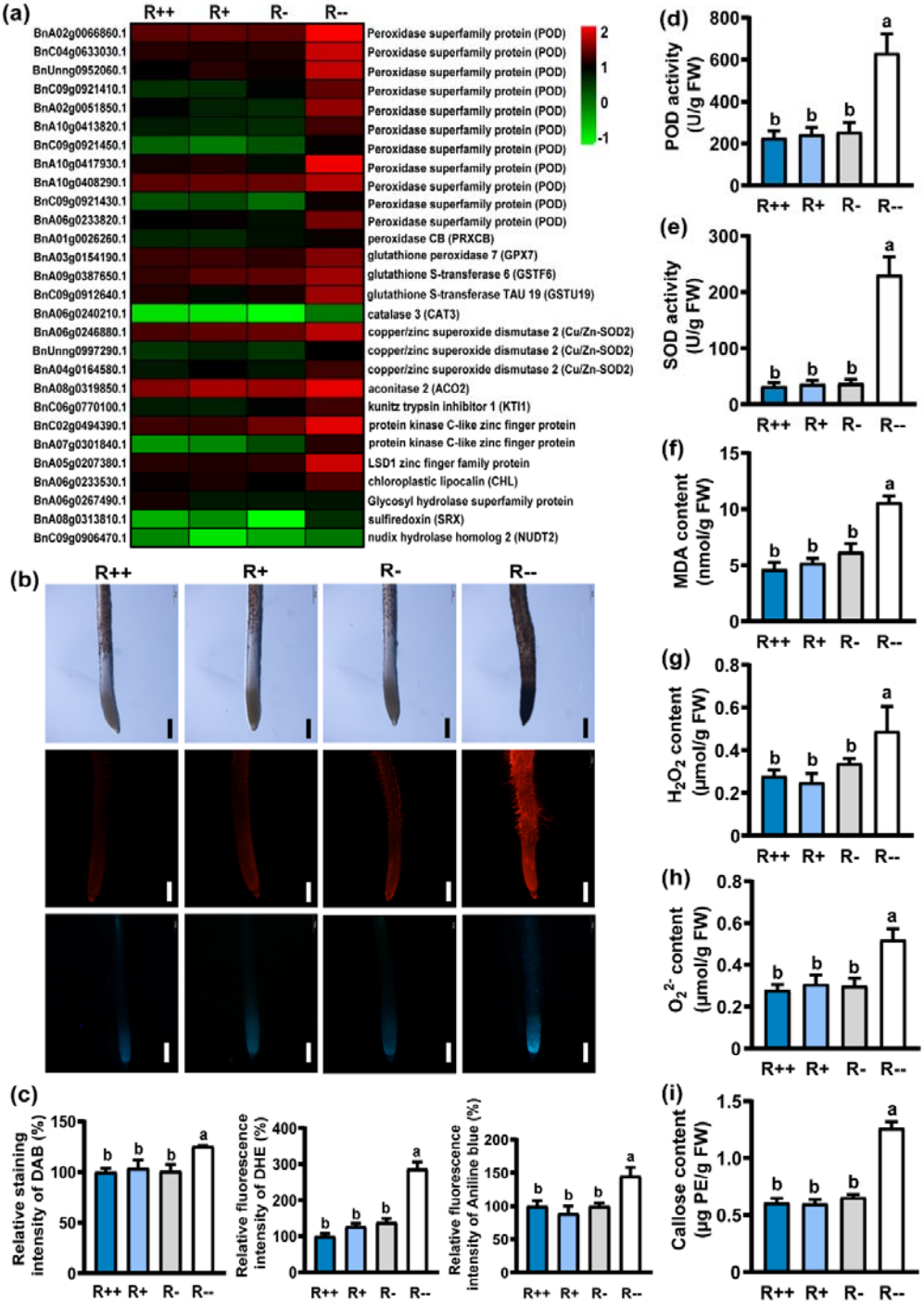

Figure 10. Modulation of the antioxidant system in roots of *B. napus* in response to Pi starvation. (a) A heatmap showing the expression of 28 differentially expressed genes (DEG), based on relative FPKM values, in the GO term of response to oxidative stress. The gene ID and gene function in *B.*

napus are shown on the left and right, respectively. The gradient colour barcode in the top right corner represents normalized FPKM values. (b) In situ accumulation of H_2O_2 (the upper row), O_2^- (the middle row) and callose (the bottom row) in the root tips as revealed by histochemical staining with DAB, DHE and aniline blue, respectively. Scale bar = 200 μm. (c) Quantification of DAB reactive staining intensity, relative fluorescent intensity of DHE and aniline blue in the root, respectively (n ≥ 20). (d, e) Activities of POD (d) and SOD (e) enzymes and (f) H_2O_2, (g) O_2^-, (h) callose and (i) MDA content in the root measured 9 DAT to the split-root system. Values are the means ± SE (n = 5 biological replicates, each replicate being a composite sample of 10 plants). A one-way ANOVA was carried out for the whole data set, and post hoc comparisons were conducted using the SPSS Tukey HSD test at $P < 0.05$ level. Significant differences were indicated by different letters above each column.

Figure 11

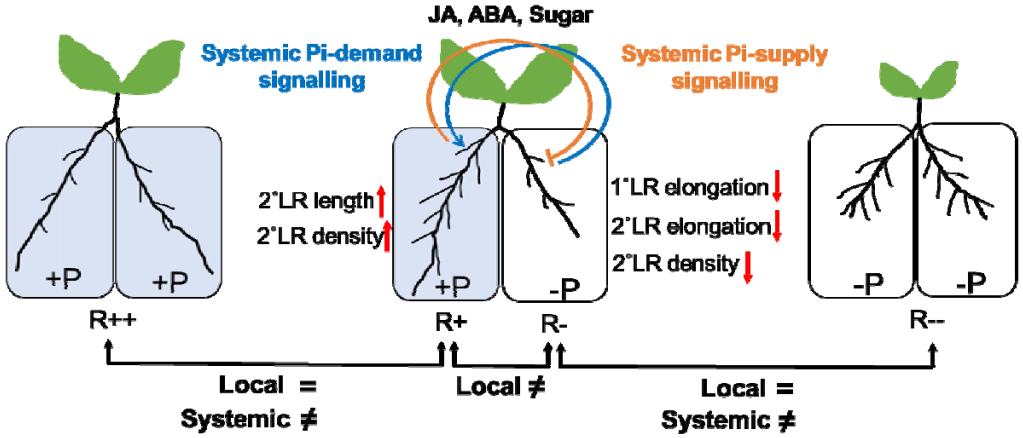

Figure 11. Schematic model for local and systemic signalling involved in RSA of *B. napus* response to homogeneous and heterogeneous Pi availability in split-root system. We speculate the existence of systemic signalling for P supply and P demand that regulate RSA exposed to heterogeneous Pi availability: systemic P-demand (−P) signalling promote 2˚LR growth of R+ (in blue), systemic P-supply (+P) signalling inhibit 2˚LR growth of R- (in orange) in split-root plants. Hormones (ABA and JA) and sugars are involved in the systemic response of RSA to Pi starvation. These systemic signallings act likely in combination with local signallings to regulate root development. "=" and "≠" indicate the expression level of genes between two groups roots are similar and significant different, respectively.